LAWRENCE
LIVERMORE
NATIONAL
LABORATORY

LLNL-TH-400176

Tailored Ceramics for Laser Applications

J. Hollingsworth

January 2, 2008

Disclaimer

This work performed under the auspices of the U.S. Department of Energy by Lawrence Livermore National Laboratory under Contract DE-AC52-07NA27344.

Tailored Ceramics for Laser Applications

Joel Hollingsworth

December 10, 2007

Contents

Abstract

Transparent ceramics match or exceed the performance of single-crystal materials in laser applications, with a more-robust fabrication process. Controlling the distribution of optical dopants in transparent ceramics

would allow qualitative improvements in amplifier slab design, by allowing gain and loss to be varied within the material. My work aims to achieve a controlled pattern or gradient of dopant prior to sintering, in order to produce tailored ceramics. This will require an understanding of dopant diffusion during sintering. I plan to investigate the neodymium-doped yttrium aluminum garnet (Nd:YAG) system, developing fabrication techniques and measuring Nd diffusion rates, with the goal of building a general diffusion model for this system. The results of experiments in green body fabrication will be included in the data that guide modeling, to allow that model to apply as broadly as possible.

Part I
Background

1 Laser ceramic basics

Transparent ceramics are fabricated by sintering high-purity powders to form a fully-dense polycrystalline body with a cubic crystal structure. Any significant birefringence, phase inhomogeneity, or porosity would scatter light, making the material translucent. Several decades of improvement, detailed in section 2, have resulted in ceramics that are transparent enough to be used as gain media for lasers.

1.1 Advantages of laser ceramics

Transparent ceramics can match or exceed the performance of single crystals in laser applications. For instance, Nd:YAG ceramics have been produced with scattering coefficients of less than 0.15%/cm, which is better than the 0.2-0.4%/cm observed in Nd:YAG single crystals grown by the Czochralski method[1].

Ceramic amplifiers have many advantages over single crystals, including greater mechanical toughness[2], less residual stress, better optical homogeneity[3], and fewer constraints on dopant distribution and solubility.

The increase in toughness is due to microstructure: grain boundaries within ceramics frustrate crack propagation, making the material less brittle and better-able to withstand mechanical damage.

Small grains also prevent defects such as twin boundaries from extending far enough to significantly degrade optical properties, resulting in better overall homogeneity.

Another source of optical defects in single crystals is residual stress, which arises from the thermal gradients that cause crystals to grow from molten material. A difference in thermal contraction at different parts of the boule causes elastic strain to be frozen into crystal amplifiers, leading to small but significant optical effects. By contrast, a ceramic slab is sintered at a very nearly constant

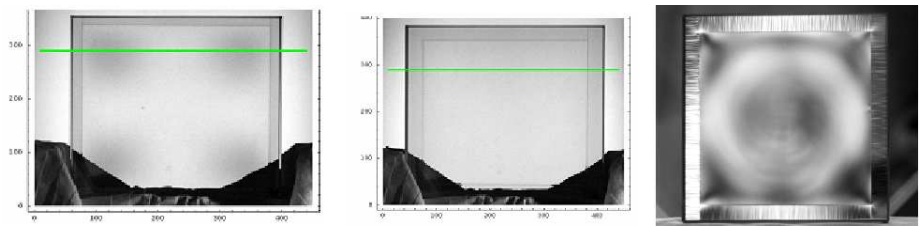

Figure 1: A comparison of optical homogeneity between ceramic (left, center) and single-crystal (right) amplifier slabs. All slabs are shown between crossed polarizers.

temperature throughout its volume, and the large volume change that occurs due to sintering allows for a nearly complete release of residual stress. Figure 1 shows some examples of the optical homogeneity of ceramics versus single crystals.

The growth of single crsytals also places constraints on the distribution of optical dopants. The solute concentration profile of a single crystal grown from a melt is dictated by the segregation ratio for that particular crystal-solute pair. This ratio is only 0.18 for Nd^{3+} in YAG[4]. Rejection of solute into the melt causes a concentration gradient in melt-grown crystals, theoretically in the form shown in figure 2. Since laser ceramics are formed without melting, they can be made witha uniform concentration. An increase in solubility below the melting point also allows Nd concentration in ceramics to be higher than is achievable in a high-quality single crystal[2].

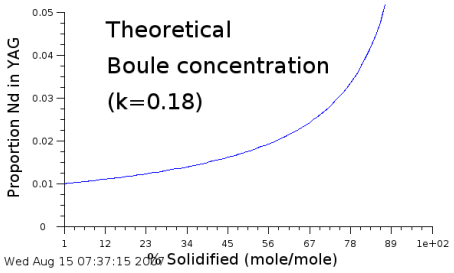

Figure 2: Theoretical concentration profile due to solidification from a perfectly-mixed melt, with no solid-state diffusion and a rejection ratio of 0.18.

While greater uniformity is possible in ceramics, a controlled nonuniformity of optical dopants is also an option; it is perhaps the most exciting option offered by the development of laser ceramics. A ceramic green body can have an arbitrary concentration profile, and will remain solid during subsequent processing. This raises the possibility that a laser designer could specify a doping profile, and sinter a solid-state amplifier which is tailored to the needs of the

laser system.s

2 History of transparent ceramics[1]

2.1 Early commercial translucent polycrystalline alumina ceramics

The first commercial translucent ceramic was a fully-dense PCA developed by the General Electric Company and trade-named Lucalox(tm). It was patented in 1962[6] and has been extensively used as the discharge envelope for high-pressure sodium lamps. Although not transparent, it diffusely transmits the sodium discharge light. More recently it is also being used as the discharge envelope for high-pressure metal-halide lamps, which, because of their high color rendition, are being used in both indoor and outdoor applications. The key to the development of nearly pore-free PCA was the addition of magnesia as a dopant to inhibit grain growth during sintering[7]. Earlier work on alumina showed that pores are closed during the final stages of sintering by material transported from grain boundaries via bulk diffusion[8, 9]. In traditional ceramics, grains often envelop pores during rapid growth, and the bulk diffusion path to remove them is too long for a practical rate of sintering to continue[10].

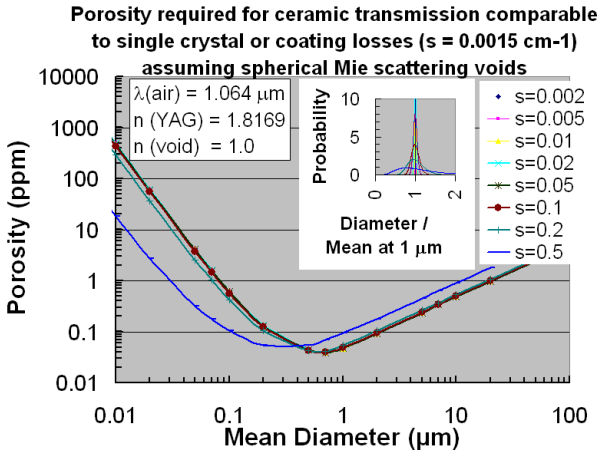

Figure 3: Acceptable porosity in YAG laser amplifiers

Lucalox is fabricated by starting with a high purity alumina powder, such as that produced by Baikowski International through the ammonium alum process. The alumina powder is thoroughly blended with a suitable organic binder

[1]Section 2 is adapted from recent work by the author[5], in press at the time of writing. Major additions to section 2.5.2 appear here, but the remainder of the section is largely unchanged.

and a few hundred parts per million (ppm) by weight magnesia. Tubes or other parts are extruded and, after baking out the binder at around 1100 ℃ in air, the parts are sintered at ~1800 ℃ in an atmosphere of hydrogen for six hours[6]. Peelen[11] showed that PCA with quality similar to Lucalox could also be made by hot pressing alumina.Although the porosity in Lucalox is very low, on the order of 0.1 to 0.01 %, it is still too high for transparency. Soules[12] and later Peelen[13] showed through Mie scattering calculations, similar to those shown in figure 3, that the optical properties of PCA could be explained by the remaining porosity. Soules also showed that the birefringence of alumina and the presence of magnesia dopants would cause rays to deviate, but would not be an important contributor to the reflectance of the material.

Transparent MgF_2 ceramics were first formed by vacuum hot-pressing this material. The process was patented[14] and used for making missile domes transparent in the infrared. Vacuum hot pressing of transparent CaF_2[15], LaF_3[16], MgO[17, 18], ZnO[19], ZnS[20] and other materials was developed and patented in the period between 1964 and 1968. W. F. Parsons[21] reviewed the history of optical elements made by hot pressing up to 1972.

By the late 1960s, two groups reported fabricating transparent yttria (Y_2O_3) ceramics by hot forging. Brissette et al.[22] thermo-mechanically deformed a pressed powder sample of yttria heated to 100 ℃ below sintering by pressing it without a die. They observed anisotropy in the grain orientation and showed higher transparency in the forged sample compared to a sample pressed uniaxially with a die. Lefever et al.[23] started with yttria powder ~ 3 μm in size and milled it with 3-5 wt % LiF. The powder was first cold pressed and then subjected to a vacuum hot press similar to Brissette et al. When the temperature reached 850-900 ℃ and pressure 8.3 MPa, the die broke and the forging began. The pressure was ramped to ~80 MPa and held for 12 hours. The workers claimed good transparency with transmission close to that of a single crystal. Dutta and Gazza[24] also produced yttria ceramics with good transparency by hot pressing. The important processing conditions were the temperature at which pressure was applied, the heating rate and the use of a non-reactive spacer material between the anvil and the sample. Anderson[25, 26] developed YttraloxTM, a transparent yttria based ceramic containing also 2-15 mol % ThO_2, ZrO_2 or HfO_2. As in the case of LucaloxTM the dopants were grain growth inhibiters. Yttralox was prepared by first thoroughly mixing the powders, cold pressing at 70 MPa and then sintering in hydrogen in a Mo strip furnace at 2000 to 2200 ℃ for four hours with no external pressure.

2.2 The first laser ceramics (1964-1975)

2.2.1 Fluorides

Hatch, Parsons and Weagley[27] at Eastman Kodak Company were the first to report laser amplification from polycrystalline ceramics, Dy2+:CaF2 and Dy2+:SrF2. The fluoride ceramics were prepared by first vacuum melting the desired portions of CaF2 and DyF2 and then pulverizing the solidified material

to ~150 μm. The ceramics were fabricated by vacuum hot pressing similar to that described in the references above. The ceramic Dy2+:CaF2 was transparent and exhibited laser oscillation at cryogenic temperatures. However, performance was not as good as for single-crystal Dy2+:CaF2 lasers. Lower efficiency was attributed to scattering by very fine inclusions of perhaps CaO.

2.2.2 Yttria

The first polycrystalline oxide laser was Yttralox, with ~ 10 % thoria as a grain growth inhibitor and 1 % Nd_2O_3 as the optically-active dopant ion, reported by Greskovich and Chernoch[28] in 1973. Appropriate amounts of the nitrates were dissolved and dripped into a solution of oxalic acid to co-precipitate a mixed oxalate salt, which was washed and calcined to form an oxide powder. The powder was cold pressed, then sintered in dry hydrogen (dew point 70 °C) for 6 hours at 2170 °C[29]. They emphasize the importance of ball milling the powder before sintering to decrease porosity. Pore densities were measured by counting pores observed under an optical microscope and were typically less than one to a few ppm[30]. Unfortunately, laser slope efficiencies were much lower than expected and laser thresholds were higher. They attributed the low laser efficiency to local variations in the material's index of refraction[31]. After these early studies a number of other authors have attempted to make use of a second phase during sintering. Additives studied included BeO[32], Al_2O_3[33], MgO[33], La_2O_3[34, 35], and LiF[36]. Some of these were chosen to be transient phases, which would influence the sintering process and subsequently evaporate or re-dissolve.

2.3 Transparent ceramics (1975-1995)

Following the work of Greskovitch and Chernoch there is a dearth of publications using transparent ceramics for lasers until 1995. In the meantime, however, there were a number of developments in the field of transparent ceramics that impact the preparation of later laser ceramics.

2.3.1 AlON

The optical anisotropy of non-cubic materials, such as α-alumina, will distort a beam of light passing through randomly oriented grains. However, the addition of aluminum nitride stabilizes the cubic γ-phase of alumina to form a material known as AlON or nitrogen-stabilized cubic alumina. There is a relatively wide range of compositional stability centered at $5AlN{\cdot}9Al_2O_3$[37]. To make transparent ALON ceramics α-alumina is ball milled with AlN in ethanol for 12 hours. It is then isostatically cold pressed and pre-reacted at 1200 °Cfor 24 hours. Sintering is carried out at 1975 °Cin a BN-covered crucible. McCauley and Corbin[37] carried out a systematic study of phase equilibria for the AlN-Al_2O_3 system in flowing N2, and, in the process, produced a translucent material. The Raytheon Company significantly improved the transparency of

AlON ceramics by optimizing the process and adding a small amount of yttria (~ 600 ppm) and ~ 100 ppm boron from crucibles[38]. Raytheon's ALON(r) has been made in large pieces for use as missile windows and transparent armor.

2.3.2 Spinel

Another important transparent ceramic material considered for infrared missile windows and transparent armor is spinel, $MgAl_2O_4$. The first reports of translucent spinel are from 1974. Bratton[39] calcined a Mg/Al hydroxide coprecipitate (CP) at 1100 ℃ for 4 hrs. The powders were screened (~200 mesh), ball milled and calcined at 1100 ℃. A small amount of calcium, 0.5 - 1.0 wt %, was added by mechanically blending the powder in a calcium nitrate, sulfate or chloride salt solution, drying and again calcining to remove the volatile anions. Sintering was carried out first at 1500 ℃ in vacuum and then 1750-1850 ℃ in vacuum or Ar.

Since these early studies there have been numerous syntheses reported of spinel. In addition to using different high purity sources of Mg and Al, different sintering and compacting techniques have been used. Hot pressing[40] achieved better results than those quoted above for sintering without pressure. Hot pressing of transparent spinel generally requires adding a small amount (~ 2 wt %) of LiF as a sintering aid[41]. Villalobos, et al.[42], at the Naval Research Laboratory claimed that to fabricate spinel to high transparency reproducibly required a homogenous distribution of LiF in the precursor material. LiF must also volatilize out of the material, which can limit the thickness of a finished ceramic body.

Sample preparation by Li et al.[43] began with co-precipitation of a mixed carbonate. An aqueous solution of high-purity aluminum and magnesium nitrates was added drop-wise to a 0.15M solution of NH_4HCO_3 with stirring at 50 ℃. The solution was aged for 12 hr and then suction filtered, washed, rinsed with ethanol and dried. The powder was isostatically pressed and vacuum sintered for 2 hrs. Shimada et al. used commercial spinel, magnesia and alumina powders, ball milled together for 16-64 hours, isostatically pressed, sintered, and further densified in a hot isostatic press (HIP)[44, 45]. HIPing was relatively new to ceramic fabrication. It involves a two stage process. First the green structure is sintered in a high vacuum to ~ 92 % of theoretical density to close pores. The closed-pore sintered part is placed in a high-pressure vessel, and the vessel is heated and filled with typically 200-400 MPa of Ar. The high hydrostatic pressure closes residual porosity.

Bickmore et al.[46] developed a flame spray pyrolysis (FSP) technique for making various ceramic raw materials. For spinel, a double alkoxide metal-organic is prepared by heating a suspension of the Al and Mg oxides or hydroxides in triethylamine and ethylene glycol at 200 ℃. After complexation, the solution is mixed with alcohol and fed into an oxygen-natural gas flame. The result is spherical $<$30 nm sized non-agglomerated particles that are collected by means of an electrostatic precipitator. This type of precursor will be discussed in more detail in a later section. Due to its high surface area and

non-agglomerated nature the powder is "active" in sintering. This attribute, combined with a high-pressure, low-temperature sintering, allowed the development of a transparent material with grains less than 100 nm in size[47].

2.3.3 Yttria

Vacuum-sintering followed by HIPing was also applied to yttria, producing 80% in-line transmission without the need for any sintering aid. However, even when the initial vacuum sintering was kept to as short a time as possible, some reduction of the oxide occurred, and annealing in air was necessary to recover transparency[48]. This process was refined to include a grog of oxides, such as ZrO_2, to prevent reduction in the HIP vessel[49]. Hot pressing at lower temperatures, followed by a slightly higher-pressure HIPing step yielded better-quality yttria without any reported reduction of the oxide[50]. In a very recent attempt at second-phase sintering, Belyakov[51] used 6 mol % hafnia to pin grains during the sintering of yttria. An in-line transmission of 64% was achieved via vacuum sintering. Raytheon has developed yttria, spinel, and ZnSe windows large enough for missile domes and other government applications[52]. The yttria windows were made by starting with 99.99 % yttria powder, milled so that there were no agglomerates and an average particle size of 1-2 μm, and formed in a Teflon-coated mold placed in an isostatic press. The green body was heated to 1350-1450 ℃ to drive off volatile substances such as dispersants. It was sintered at a temperature of 1800-1900 ℃ to achieve closed porosity and then HIPed for 1/2-10 hours at a temperature of 1700-1900 ℃ and a pressure of 170-200 MPa. The sample was later annealed in air at 1400-1800 ℃ to remove discoloration due to reduction[48].

2.3.4 ZnSe and other windows

ZnSe is the most commonly used optical window for infrared radiation with $\lambda = 5 - 20\mu m$. Transparent ceramic parts are commercially available, prepared by reacting H_2Se with zinc vapor in a chemically vapor deposition (CVD) process. Certain other materials, for example SiAlON[53, 54, 55, 56, 57, 58], LiAlON[59], aluminum magnesium oxynitride[60, 44] silicon nitride[61, 62] and aluminum nitride[63, 64, 65, 66] have been made translucent to transparent for potential window applications.

2.3.5 Scintillators-Eu^{3+}-doped rare-earth sesquioxides

Since the early 1980s transparent ceramic scintillators have been progressively replacing single crystals in modern digital detectors, such as those on X-ray computer aided tomography (CAT) scanners and positron emission tomography (PET) scanners. Ceramics have many advantages over single crystals for scintillators. They provide much broader range of materials and are easier to fabricate. Scintillators for tomography absorb X-rays or gamma rays throughout a bar 1~3 cm long and a couple mm^2 in cross section, which serves as one pixel. The

ionizing radiation excites luminescent dopant centers throughout the bar and is converted, through relaxation and emission to a wavelength suitable for a silicon or other detector. The emitted radiation must be effectively transmitted by the bar to the detector at one end, but some amount of scattering can be accepted (attenuation coefficients < 100 % /cm). General Electric developed a transparent scintillator material with composition $Y_{1.34}Gd_{0.6}Eu_{0.06}Pr_{0.0001}O_3$[67] for its CAT scan systems. Gadolinia forms a solid solution with yttria up to ~40 at % while keeping the cubic bixbyite structure, and is added for its higher X-ray stopping power compared to Y. Eu^{3+} is the luminescent dopant or activator. It has near-unity quantum efficiency in yttria/gadolinia, and emits in a single narrow band at 611 nm: a good match to a silicon detector. Pr^{3+} or certain other dopants are added in small amounts to suppress afterglow, which is important since the detector bar will be addressed in every pass of the X-ray beam. This scintillator ceramic was developed over several years. According to the patent, it is fabricated by blending high purity yttria and gadolinia submicron powders with the desired rare-earth activators in the form of oxides. Alternatively, the inventors claim that the powder can be prepared by dissolving the appropriate amount of the nitrates in water and then adding this to a solution of oxalic acid, 80 % saturated at room temperature. The co-precipitated oxalates are washed, neutralized, filtered and dried in air and then calcined at 800 ℃ for 1 hour. The powder is then ball milled or fluid-energy milled to break up aggregates that would cause porosity in the final product. The green structure is prepared by cold pressing the powder and then isostatically pressing to further increase the green density. The green body is sintered at 1800-2100 ℃ in vacuum or wet hydrogen (dew point 23 ℃) for between 1 and 30 hours. Alternatively the powder may be pre-sintered at 1500-1700 ℃ to achieve closed porosity at 93-98 % of its theoretical density and then HIPed at 1750 ℃[68]. The resulting ceramic is black due to reduction but is rendered transparent by heating in air at 1200 ℃ for thirty-two hours. Yttria/gadolinia scintillators can also be prepared by hot pressing. If the oxalate precipitate is further refined by agitating an aqueous suspension while admixing an effective amount of ammonium hydroxide to increase the pH to 8-10, then it is possible to prepare the scintillator material by pressureless sintering at between 1800 and 2100 ℃ in wet hydrogen[69, 70]. Lu_2O_3:Eu^{3+} has a still-higher X-ray stopping power than yttria-gadolinia, and was studied as a highly efficient scintillator for digital radiography and fluoroscopy[71]. Both laser and scintillator materials were produced by co-precipitation of rare-earth nitrate solutions using oxalic acid. After washing and calcinations the green structure was hot pressed, and then heated in air for 2 hours at 1200 ℃ to remove reduction discoloration.

2.3.6 Scintillators-Gadolinium oxysulfide:Pr^{3+}

Transparent ceramic $(Gd_{0.999}Pr_{0.001}Ce_{0.0001})_2O_2S$ was developed by the Siemens Company for X-ray tomography about the same time as yttria-gadolinia. Because it is not cubic there is some refraction, reflection and birefringence at grain boundaries. However it can be made transparent enough for the CAT

scanner. The oxysulfide is prepared starting with a water suspension of the appropriate amounts of the oxides. One mole of sulfuric acid is added per mole of rare earth ions. The reaction is carried out at a temperature around 70-100 ℃ for 5-200 minutes. The precipitate, a rare-earth oxysulfate, is washed, filtered, dried and calcined. Then the oxysulfate is reduced to the oxysulfide by firing in a reducing atmosphere of hydrogen, carbon monoxide, or other reducing gas at between 500 and 1000 ℃[68]. According to the inventors the transparent ceramic can be produced by uniaxial hot pressing, HIPing or sintering without pressure. Matsuda[72] suggests sealing the green structure in a flexible metal envelope made of tantalum or niobium before performing the HIP at 1300-1800 ℃. A good review of scintillator materials including a comparison between ceramic scintillators and single crystals up to 1997 is given by Greskovich and Duclos[1].

2.3.7 High energy ceramic scintillators

Recently there has been considerable interest in scintillators for high energy gamma rays and positron emission tomography (PET). These scintillators must have very short decay times and recovery times. Ce^{3+} is the activator of choice because it efficiently luminesces in several hosts, and because the allowed d-f transition has a lifetime on the order of tens of nanoseconds, depending on the host. In 1996, General Electric patented a method for making ceramic garnet scintillators with the chemical formula $A_3B_5O_{12}$ including gadolinium gallium garnet ($Gd_3Ga_5O_{12}$), gadolinium scandium gallium garnet ($Gd_3Sc_2Ga_3O_{12}$), and gadolinium scandium aluminum garnet ($Gd_3Sc_2Al_3O_{12}$)[73] with Cr^{3+} or Ce^{3+} or Nd^{3+} ions as activators. To prepare these ceramics, the oxides were dissolved in hydrochloric acid and then precipitated as hydroxides by drop-wise addition of ammonia, until the pH was in the range of 7.8-8.3. The precipitate was washed, rinsed with alcohol, dried, calcined at 900 ℃, cold pressed and isostatically pressed. The green structure was sintered in an oxygen atmosphere at 1400-1600 ℃. These ceramic scintillators showed more loss than single crystals, transferring energy to defects, perhaps at grain boundaries[73]. Lutetium aluminum garnet, $Lu_3Al_5O_{12}$ (LuAG), is a promising scintillator host having high X-ray and gamma ray absorption due to the high atomic number and density of Lu. Lutetium silicate (Lu_2SiO_5) doped with Ce has also been sintered as a scintillator[74]. Very transparent ceramic slabs of LuAG materials have been produced by using a carbonate precipitation similar to that discussed for laser ceramics in the latter half of Section II, 4 (A). Lutetia is dissolved in nitric acid and added to a solution of aluminum nitrate. The mixed nitrate solution is added at 2 ml/min into 2M ammonium hydrogen carbonate solution under mild stirring. The resulting precipitate is filtered, washed, dried and calcined as above and isostatically pressed into a green structure. Sintering is carried out at 1850 ℃ for 6 hours in a hydrogen atmosphere. The advantage of the carbonate precipitate is small particle size and little agglomeration resulting in quite transparent parts[75]. Ce-doped LuAG was also made via reactive sintering, by ball milling very pure lutetia, alumina and ceria in the correct proportions in alco-

hol and then sintering the pressed blended oxides in a vacuum at 1760 ℃ for 10 hours, followed by annealing at 1450 ℃ for 20 hours[76]. LuAG was also made via reactive sintering, by ball milling very pure lutetia, alumina and ceria in the correct proportions in alcohol and then sintering the pressed blended oxides in a vacuum at 1760 ℃ for 10 hours, followed by annealing at 1450 ℃ for 20 hours78. Kuntz[77] compared the reactive sintering method of Li et al.[76] with FSP produced LuAG. Both materials were vacuum sintered for 8 hours at 1800 ℃. The FSP route led to significantly improved optical properties. Today, cerium-doped YAG with very good transparency can be purchased commercially.

2.3.8 Transparent ceramic electrooptics

Another area of interest in lasers is optical switching. Transparent ceramic electrooptic materials-solid solutions of the perovskites: lead zirconate, lead titanate and lanthanum zirconate, i.e. (Pb, La)(Zr, Ti)O_3 or PLZT-have been studied for almost 40 years[78, 79, 80]. Transparent ceramic PLZT has advantages over competing technologies, such as liquid crystals, in simplicity of construction and fast response. A disadvantage is the relatively high voltages required for switching. PLZT is fabricated either by blending and ball milling appropriate amounts of the high purity oxide powders, PbO, ZrO_2, TiO_2 and La_2O_3 (a mixed oxide (MO) process), or by an organometallic process. The latter process involves starting with high-purity liquid tetrabutyl zirconate and tetrabutyl titanate, which are mixed with lead oxide in a high-speed blender and then precipitated by adding a water solution of lanthanum acetate. The slurry is dried, calcined, wet milled and cold pressed prior to sintering[81]. Haertling and Land[79] were the first to achieve transparency in ferroelectric ceramics. This group achieved 80% transmittance in an 8% La sample via hot pressing, with a refractory powder such as magnesia around the part to prevent reaction with surrounding materials, at 1100-1300 ℃ and 14 MPa for 10 hours. Snow[82] showed that excess PbO_2 could be used to create a liquid phase during sintering, allowing translucent materials to be fabricated by a pressureless sintering process. This required a sintering atmosphere rich in O_2 and PbO_2 vapor, and a controlled rate of PbO_2 evaporation from the finished product to allow closure of the pores left by removal of the second phase. Results were not quite as good as for hot-pressing, with transmission of only 50%. More recently several other compositions have been reported based on using lead niobate in place of lead zirconate and a divalent cation to balance the charge in the perovskite structure[83]. $Pb(Mg_{\frac{1}{3}}Nb_{\frac{2}{3}})O_3$-$PbTiO_3$ (PMN-PT) has been developed, and it has much less hysteresis than PLZT. It also has an isotropic cubic perovskite structure, which can be easily distorted by applying an electric field, producing birefringence that varies quadratically with the field. The electrooptic effect is 2-5 times higher that that of PLZT and 100 times higher than LiNbO3. Nanosecond modulation has been achieved[84]. PMN-PT can be prepared by either the MO or CP process but the co-precipitation process is preferred for higher purity and a more-homogenous material. Powder preparation is most important to the transparency. The transparency achieved in OptoCeramicTM

PMN-PT at Boston Applied Technologies, Incorporated matches or is slightly better than PLZT, ~3 dB/cm attenuation at a wavelength of 1.5 micrometers. PLZT has also been studied as a laser host material. Spectroscopic studies were carried out by de Camargo et al.[85], for ceramics doped with Nd, Er, and Yb. The following year, stimulated emission was observed in Nd-doped PLZT[86].

2.4 Laser ceramic gain media (1995-2005)

2.4.1 Laser quality ceramic Nd:YAG

Nd:YAG is probably the most commonly used solid-state laser material. Single crystals are grown using the Czochralski (Cz) method. Translucent YAG ceramic was first made using SiO_2 to aid sintering or MgO to inhibit grain growth. These findings emphasized the importance of smaller, more-uniform powder grains, and recommended silicon-based additives over magnesia[87].

In 1995, Ikesue et al.[88] demonstrated transparent ceramic Nd:YAG samples with an attenuation coefficient at 1000 nm (measured by using the slope of the log of the transmitted intensity versus sample thickness) of 0.9 % / cm. This was a dramatic improvement over the transparencies of any of the ceramics discussed above, providing impetus to subsequent development of transparent ceramics for commercial lasers. Ikesue also showed a comparison of the lasing power of ceramic YAG with 1.1 at % Nd versus a single crystal doped at 0.9 at % Nd as a function of input pumping power. The ceramic had a comparable threshold for lasing, ~300 mW, and comparable lasing efficiency, ~28 %. Ikesue also showed the pore structure and the change in density during heating by interrupting heating of samples at different temperatures. A comparison of properties of the sintered ceramic versus the single crystal showed that Vickers hardness, refractive index, room and higher temperature thermal conductivity, and optical properties were essentially the same as those of the single crystal.

In the same year, Ikesue et al.[89] reported on Cr^{3+}/Nd^{3+} co-doped YAG. Cr^{3+} absorbs radiation throughout the visible region of the spectrum, making it a good absorber for flashlamps or perhaps sunlight. The energy is then transferred non-radiatively to Nd^{3+} for lasing at 1064 nm. Ueda suggested this approach for potentially a solar pumped laser[90]. Ikesue et al.[3] prepared samples by first synthesizing the oxide powders by alkoxide precipitation of Al from solution, pyrolysis of $Y(OH)_2Cl$, and oxalate precipitation of Nd. After calcinations, the Al_2O_3, Y_2O_3 and Nd_2O_3 powders were blended and ball milled using high purity alumina balls for 12 hours in alcohol mixed with 0.5 wt % tetraethyl orthosilicate (TEOS). They claim that both the small addition of silica (measured at 320 ppm in the final part) and the preparation of the raw material powders are key to obtaining their transparency. They indicate that their raw material powders are all at least 99.99 % pure and have median particle sizes of 60 to 500 nm. The slurry was dried using a spray drier with the atomizer rotation speed adjusted to give granulated spherical particles < 100 μm in diameter. Spray drying conditions can also be used to control porosity. The granulated powder was isostatically pressed into disks. Sintering was carried out for 20 to

50 hours under a vacuum of 1.3×10^{-3} Pa. Porosity was measured by microscopy was ~150 ppm. Cooling after vacuum sintering should be done rapidly at >600 ℃/hour. Ikesue et al.[91] showed that increasing the silica content and decreasing the cooling rate results in a silica-rich grain boundary phase, which decreases laser efficiency by increasing scattering in otherwise-homogeneous, low-porosity samples. Ikesue et al.[92] also tried adding a HIPing step to their process. A series of experiments were performed varying the TEOS content and varying the HIPing temperature and pressure. The results showed increased porosity due to argon being dissolved in the silicate grain boundary phase and then being released as argon gas bubbles when the pressure was released and the sample cooled.

In 1995-1996, Ikesue, et al.[93] demonstrated that the Nd^{3+} concentration could be increased from 1.1 to 2.4 and 4.8 at % in their ceramic samples. These higher concentrations are not possible in the single crystal because of the low accommodation coefficient for Nd in the YAG boule. The 1.1 and 2.4 at % samples show a somewhat higher threshold for lasing than the 0.9 at % single crystal and higher slope efficiencies. The 4.8 at % sample shows lower efficiency due to concentration quenching. However, the high concentration of Nd^{3+} is potentially useful for microchip laser applications and Ikesue, et al.97 show that for such applications, the higher Nd concentration can be up to 4 times as efficient as a 1 at % Nd single crystal. Lupei, et al.[94] studied the high-resolution spectral properties of Nd:YAG ceramics made by the above process up to concentrations of 9 at % Nd. The spectra are consistent with Nd ions occupying only the D2 sites of YAG similar to perfect flux-grown single crystals. With increasing concentration, satellite peaks are consistent with a statistical distribution of Nd-Nd next-nearest neighbor pairs, and at higher concentrations some statistical triads of three Nd ions on near-neighbor D2 lattice sites. Emission decay curves of the 1 at % ceramics are very similar to the single crystal. Decay curves at higher concentrations can be explained by energy transfer and cross relaxation with some energy migration. At higher Nd concentrations, absorption increases and the absorption bands widen, allowing Nd ions to be pumped at 885 nm rather than the usual 808 nm. 885 nm pumping would reduce the quantum defect heating of the lasing medium by ~30%[95].

Even before the Ikesue paper in 1995, a second group in Japan[96] had achieved attenuation coefficients of 2.5 - 3.0 %/cm for Nd:YAG ceramics using a different approach to the synthesis. Their approach was to first carefully prepare 1M solutions of YCl_3, $AlCl_3$, $NdCl_3$, and $(NH_4)_2SO_4$. These solutions were mixed in the ratio of 50-x/30/x/30 where x was chosen to determine Nd doping in the final oxide. Next, 72 g of urea and 0.003 g of colloidal silica were added to the solution. The temperature was raised to 95 ℃ and held for 2 hours, during which time the urea hydrolyzed and coprecipitated all the cations as amorphous hydroxides. The coprecipitate was washed, filtered, calcined, pressed into disks, and then vacuum sintered at 1700 ℃. Said group measured absorption and emission spectra of the samples with different Nd concentrations and, except for the background attenuation from scattering, the spectral features are the same as for the single crystal. The calculated induced emission

cross section was $\approx 49 \times 10^{-20} cm^2$, in reasonable agreement with values obtained from laser measurements in the single crystal. Precipitation techniques continued to improve, further reducing the level of porosity. In the year 2000, Li et al.[97] emphasized the importance of precipitate agglomeration, and compared two methods of precipitation. A solution of pure yttrium and aluminum nitrates in distilled water was divided and added to two separate solutions, one of ammonium hydrogen carbonate and one of ammonium hydroxide. The hydroxide precipitate was gelatinous and more difficult to process than the carbonate precipitate. The two precipitates were calcined in oxygen, isostatically pressed, and vacuum sintered under comparable conditions. The YAG from carbonates sintered more completely and with less agglomeration than YAG from mixed hydroxides. Using carbonate co-precipitation methods later that year, Lu, et al.[98, 99] claimed a porosity of ~1 ppm, in agreement with the theoretical calculations shown in Figure 3 and two orders of magnitude less than observed by Ikesue in his transparent ceramics. Unfortunately, it is not clear how the measurement techniques should be compared. Lu, et al.'s method of preparation of the starting powder is described in two Japanese patents [100, 99]. In the first patent, aqueous solutions of 1 M of YCl_3 and 1 M $AlCl_3$ were carefully prepared and mixed together in the 3/5 volume ratio, and concentrated sulfuric acid was added in molar ratio of 0.75 SO_4^{2-} per metal ion. 2.5 M ammonium hydrogen carbonate solution was added drop-wise to the acidic metal ion solution to achieve a pH of 4.8 (adding the precipitant to the metal salt solution is known as the normal-strike precipitation). The solution was allowed to age for 12 hr and then ammonia was added until the pH reached 7.5. By this time all metal ions had precipitated. Six rounds of filtering and washing were carried out, until the anion content of the effluent was < 2000 ppm. After drying and calcining at ~1200 ℃, a fine, well-dispersed powder was obtained, which was uniaxially and isostatically pressed, and then vacuum sintered at 1650 ℃ for 3 hours. In the second patent the precipitation order is reversed (the reverse strike method). Solutions of 0.5 M yttrium and aluminum nitrate were prepared and mixed in the proper ratios and then the metal ion solution was added drop-wise with stirring to a 2 M solution of ammonium hydrogen carbonate, keeping the pH between 7.5 and 11 with ammonia. The solution was aged until the pH stabilized in the range 7.5-11, and then filtered, washed, dried and ball milled for 24 hours, before being pressed and sintered as before. Lu et al.[98, 101] obtained 72 W of laser output from a Nd:YAG ceramic rod produced by the group at Konoshima Chemical Co., Ltd. At the time this was the highest output achieved in a Nd:YAG laser. Over the course of the next four years, decreased scattering led to further improvements in slope efficiency from 58.5% to 62%[102] and corresponding increases in laser output power. In 2002 Lu et al.[103] discussed the properties of Konoshima ceramic Nd:YAG, pointing out that stimulated Raman scattering and highly efficient laser oscillation suggested that this material would be an excellent alternative to Nd:YAG single crystals. Instead of cold pressing the powder, Konoshima was now ball milling the powder for 24 hours in alcohol and binders and pouring it into a gypsum mold (slip-casting). After drying, the slip cast sample can be removed from the mold, heated to remove

organic binders and then sintered at 1750 ℃. Ueda[104] has suggested that slip casting provides a more uniform compaction without forced local compression and possibly non-uniform density that may occur during cold pressing.

2.4.2 Laser quality ceramic Nd:YSAG and other garnets

Yttrium scandium aluminum garnet has a mix of scandium and aluminum in the octahedral sites. This variety of ion environments causes inhomogeneous broadening of the Nd emission and absorption lines, making possible a tunable laser. A ten-fold increase in the width of the Nd spectral line allows 10ps pulses to be produced[105]. Nd:YSAG can be made transparent using the mixed oxide synthesis discussed above for YAG[106]. Lasers have been made from Nd- and Yb-doped ceramic YSAG[1], showing significantly broader emission peaks.

Terbium aluminum garnet (TAG) and terbium gallium garnet (TGG) have also been made by Konoshima as Faraday rotators, a possible magneto-optical switch. TGG has one of the highest Verdet constants for a Faraday rotator and it is 40x higher at low temperatures[107].

2.4.3 Laser quality ceramic yttria, Y_2O_3

Unlike YAG, where a slight imbalance of metal ions can easily produce secondary phases, yttria does not have a second metal ion component. Several precipitation methods have been used to prepare laser quality yttria. Ikegami et al.[108] precipitated yttrium hydroxide from a solution of $Y(NO_3)_3{\cdot}6H_2O$ by adding a 2N aqueous ammonia solution at 10 ml/min and 0.36 g/100 ml of ammonium sulfate. The precipitate was aged at 10 ℃, 50 ℃ and 100 ℃. After aging the cold precipitate contains thin flakes arranged as houses of cards. The sulfate ions reduce anisotropy and result in more-spherical particles, which is reportedly essential to achieving good transparency. In 2007, Fukabori et al.[109] published a continuation of Ikegami's earlier work starting with a 0.3 M $Y(NO_3)_3$ and $Nd(NO_3)_3$ solution and adding ammonia while stirring to precipitate $Y(OH)_3$, aging, then adding a 0.05 M $(NH_4)_2SO_4$. The slurry was aged, washed and calcined as usual. They found that the sulfate should be driven off as completely as possible without forming large particles by calcining at 1080-1100 ℃. Urea precipitation was used successfully by Lu et al.[110] to fabricate Nd:Y_2O_3 and a working laser slab in 2002[111], 2003[112], and 2004[113]. The 2002 paper briefly describes the fabrication method that was presumably used in all these efforts. As in the urea precipitation discussed above, urea was added and the solution was heated to near boiling. The resulting precipitate was filtered and washed repeatedly, and dried for two days. The precursor powder was then calcined at 1100 ℃ and ball milled for 24 hours. The milled slurry was then slip cast. After organic components were removed by calcining, the green body was vacuum sintered. Saito et al.[114] described the fabrication of transparent yttria ceramics using a carbonate precipitation method. Yttrium nitrate hexahydrate (99.99 % pure) was dissolved in deionized water. A 2.5 M solution of ammonium hydrogen carbonate was dripped into the yttrium nitrate solution at a speed of

2 ml/min (normal strike). The precipitated slurry was then aged for two days, during which time the amorphous spherical carbonate crystallized and a 0.05wt % ammonium sulfate solution was added. The precipitate was filtered and washed repeatedly, and the filtered cake was dispersed in acetone and dried to prevent aggregation. The powder was calcined at 1100 ℃ for 4 hrs. It was then cold pressed and sintered at 1700 ℃ in vacuum, 10-3 Pa. In-line transmission at 1000 nm was ~50 %, compared to 80% for a single crystal.

2.4.4 Laser quality ceramic scandia, Sc_2O_3

Scandium oxide has the same bixbyite crystal structure as yttria, but higher thermal conductivity. Like yttria, Sc_2O_3 has been fabricated from several precursors. Li, et al.[115] thermally pyrolyzed scandium sulfate, $S_2(SO_4)_3{\cdot}8H_2O$ at 1200 ℃, resulting in ultra-fine Sc_2O_3 powder with good dispersion. Transparent ceramics obtained had in-line transmittance of 56-58 % in the visible. After trying several other precipitation methods, Li, et al.[116] obtained the best results by precipitating the basic sulfate, $Sc(OH)SO_4{\cdot}2H_2O$, by mixing a 0.4 M scandium nitrate solution and an equi-volume solution of ammonium sulfate. The precipitate was washed repeatedly with distilled water until free SO_4^{2-} was no longer detected with $Ba(NO_3)_2$. The powder was calcined at 1000 ℃, and was quite transparent after vacuum sintering at 1700 ℃. The urea precipitation method discussed above, followed by slip casting and vacuum sintering at 1700 ℃ for 5 hours, was used by Lu, et al.[117], who showed that the spectral properties of Yb:Sc_2O_3 are quite similar to those of Yb:Y_2O_3, and produced a laser output of 0.4W.

2.4.5 Laser quality ceramic lutetia, Lu_2O_3

Lutetia is also similar to yttria both in crystal structure and chemistry. However, the lutetium ion is very close to Yb in both size and mass, so that the addition of Yb has little effect on the thermal conductivity. This gives Yb-doped lutetia the highest thermal conductivity of any of the oxide laser materials. Lu et al.[118] fabricated Nd:Lu_2O_3 using the urea process and demonstrated laser action. The spectroscopy is very close to Nd:Y_2O_3 with just a small shift, approximately 1.5 nm, due to the different crystal field and slightly narrower line widths. Kaminski et al.[119] demonstrated efficient lasing using Yb:Lu_2O_3 ceramic samples presumably obtained using the same urea process. They also analyzed phonon transmission and scattering at grain boundaries using the heat-pulse technique at liquid helium temperatures.

2.4.6 Recent work on fluoride laser ceramics

Fluorides have certain advantages as laser gain media due to their large band gap and low non-linear optical coefficients, high quantum efficiency due to low phonon coupling and relatively low-energy phonons, and long rare-earth laser lifetimes. These advantages must be traded against difficulties in sintering transparent fluoride ceramics. Fluorides may be contaminated by water or oxygen

impurities from the air, and are typically purified under fluorine or anhydrous hydrofluoric acid. Fluorides also cannot be slip cast. Also, although they sinter at lower temperatures than oxides, they have a significant vapor pressure at sintering temperatures and so cannot be vacuum sintered without a loss of much of the material. Recently Aubry et al.[107] reported on the synthesis of ceramic CaF_2 powder via several techniques to prepare the starting powders, including reverse micelle precipitation, hydrofluoric acid precipitation, and mechanical alloying of crushed single crystals. All three methods produced a powder that was phase pure by X-ray diffraction, but sintering revealed traces of zirconia in the powder prepared by mechanical milling and organic impurities in the reverse micelle samples. Translucent parts were fabricated using uniaxial hot-pressing, spark-plasma sintering and vacuum sintering followed by HIPing.

T. T. Basiev et al.[107] reported on ceramics and single crystals of a solid solution, Yb^{3+}:(1-x)CaF_2-(x)SrF_2 (x = 5at%). They argue that, being near a eutectic composition of ~25% SrF_2, this solid solution can have better crystallinity, higher pump light absorption, and narrower spectral peaks. They report 0.9 % /cm loss in the ceramic sample and laser slope efficiency ~80 % that of the single crystal.

2.4.7 Laser quality ceramic zinc selenide, ZnSe

Cr2+:ZnSe ceramics were recently prepared by mixing CVD ZnSe and CrSe (1 at %) and hot pressing. Efficiencies of 10, 5 and 3 % were achieved for low and high doping densities. This materials system potentially offers tunable mid-IR laser light[120].

2.5 Engineered laser ceramics (2005-present)

Perhaps the most exciting advantage of transparent ceramics for the laser designer is the ability to tailor ceramics to meet the needs of the laser.

2.5.1 Co-sintered parts

Composites have been fairly recently fabricated by bonding partially-sintered ceramics. The approach is to partially sinter several parts, then polish the sides to be bonded to $\lambda/10$ flatness, with no defects under 10× magnification. The parts are then placed in contact and held under pressure during the next sintering step. Konoshima has successfully used this technique to produce Nd:YAG amplifiers clad in pure YAG. Kracht et al.[121] designed a composite cylindrical rod in which only the core was doped. The cladding internally reflected pump light and distributed it uniformly over the doped region. The rod and cladding also served as a thermally self-focusing wave guide. The design was modeled and optimized for optical absorption efficiency using a ray tracing code. With water cooling of the outside of the rod and 290 W of input power, they were able to achieve 144 W of output power, for a 64 % optical-to-optical efficiency. Strasser[122] showed that beam clipping at the aperture could be avoided by

the use of undoped cladding, using core-doped rods by Konoshima in a side-pumped configuration. Dong et al.[123] co-sintered a short rod of Cr^{4+}:YAG to Yb^{3+}:YAG to produce a single-piece Q-switched laser with a pulse energy of 125 mJ, a pulse width of 1.2 ns, and a repetition rate of 105 kHz.

2.5.2 Engineered green structure

Tailoring the powder compact before sintering would allow considerable additional flexibility in design of monolithic transparent parts. For example, a concentration gradient of Nd in YAG can be achieved by cold-pressing successive layers of powder with different concentrations of dopants[107].

Wisdom[124] identifies four potential design goals for activator profile tailoring, each with progressively less-stringent requirements for profile control: Longitudinal mode control, wave guide construction, thermal management, and transverse mode control.

Longitudinal mode control would strive to selectively amplify certain modes of oscillation, with heavier doping at the peaks of standing waves, and lighter doping at the nodes. To reap the full benefits of such a tailoring strategy would require doping to be controlled with a spatial accuracy finer than the wavelength of emitted radiation.

Wave guides could be constructed by exploiting the effect of activator doping upon refractive index, with the goal of confining light to a thin layer for more efficient amplification. This requires composition control at a length scale on the order of one wavelength, or slightly larger.

Thermal management of end-pumped rods could be accomplished by balancing the active material's absorption to the expected intensity of pump light. This would allow for uniform heating of the rod, even as different portions of it are exposed to different amounts of energy. This improved uniformity of thermal load would reduce the risk of thermal shock. This strategy calls for control of ion concentrations and gradients on a length scale of several millimeters.

Lastly, large aperture slabs may benefit from transverse mode control, which would be accomplished in much the same way as longitudinal mode control. However, the length scale of intended transverse modes is several orders of magnitude greater, allowing this goal to be met even if doping can only be controlled on a length scale of centimeters. One laser application seems particularly well suited to this strategy: edge-pumped amplifier slabs. A uniformly-doped slab will absorb more pump light at its edges than at its center, since the pump light will be dimmed by its passage through the material. This means that the edges of such a slab recieve the most pump energy, energy that is wasted amplifying the edges of the beam. If tailored ceramics can be made with well-controlled concentration gradients, then edge-pumped amplifier slabs can be made so that each point absorbs only as much pump light as is needed to amplify that portion of the beam by the desired amount.

Wisdom fabricated a waveguide structure by reactive sintering, with higher-index Nd:YAG sandwiched between lower-index undoped YAG ceramics. His design called for a 400 μm wide doped region, which was predicted to be achiev-

able based on the bulk diffusivity of Nd in YAG. However, the observed Nd diffusion distance was approximately 250 μm. Additionally, some regions showed pronounced differences between the Nd concentration near grain boundaries and that near the center of grains, which indicates the action of a high-mobility path. He attributed this rapid diffusion to the presence of transient phases that had not yet fully reacted to form YAG, based partly on the observation that a much lower diffusivity is observed during the final stage of sintering: samples sintered for 10 hours, 50 hours, and 125 hours showed identical concentration profiles.

Messing[107] presented a similar idea, using tape casting to build up layers of different concentrations of Er:YAG as a means of thermal management. Each layer is ~100 micrometers in thickness. These initial efforts have shown promising optical quality. The Er diffusion distance was on the order of 0.2 mm, and, as for Wisdom, some non-uniformity of concentration was observed when mapping fluorescence[124].

2.5.3 Single crystal growth in polycrystalline ceramics

Scott et al.[125] first observed "solid-state crystal conversion" (SSCC) in Lucalox grade polycrystalline alumina with low MgO concentration. He showed that $\approx \frac{1}{3}$ of a PCA tube with an OD of 5 mm could be converted to sapphire by soaking at 1880 ℃for 18 hrs. In an article discussing a number of experiments in engineering transparent ceramics for lasers, Ikesue111 discusses the conversion of ceramic YAG to a single crystal by polishing both a ceramic and a single crystal, putting them in contact and soaking at high temperature. Abnormal grain growth reached 1.7 mm/h at 1840 ℃. The importance of this work is that an optical-quality single crystal is obtained, and one can produce a Nd:YAG single crystal with heavier doping than is possible by melt-growth methods such as Cz.

3 Atomic mobility in YAG ceramics

The wide range of applications for YAG have prompted many investigations of diffusion in this particular material. Also,

3.1 Microstructure evolution during sintering

Several models for sintering have been devised, both analytical and numerical. All models begin with the minimization of surface and interfacial energies as the driving force for sintering, and go on to outline mechanisms for material transport, such as evaporation and condensation, viscous flow, and bulk diffusion. While a complete discussion of this subject is beyond the scope of this prospectus, some examples have been important in shaping the goals of this research.

Analytical sintering models generally separate the process into three stages, illustrated schematically in figure 4. In the first stage, the contact area between

any two grains is too narrow to allow any coarsening. In the second, some coarsening occurs, as tube-shaped pores continue to shrink. In the final stage, isolated pores with a roughly spherical shape continue to shrink, especially if they remain near grain boundaries[10].

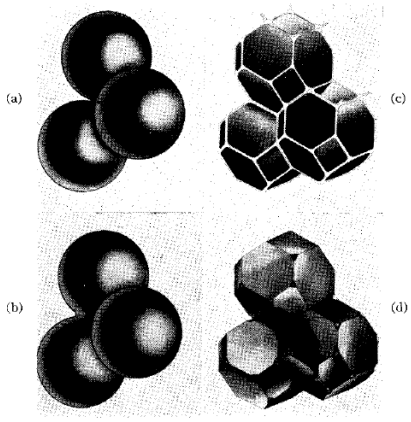

Figure 4: Schematic illustration of the three stages of sintering: (a) tangential contact between powder grains (b) neck growth; first-stage sintering (c) tube-shaped porosity (white); second-stage sintering (d) isolated tetrahedral pores; final-stage sintering. From Coble[10].

Coble[10, 7] tested a wide variety of analytical models against the observed behavior of alumina, and found that the functional dependence of density and grain size as a function of time were consistent with the model of Kingery and Berg[126], in which a bulk diffusion mechanism controls the early stages of sintering, and with the work of Burke[9], which strongly suggested that pore closure during the final stage of sintering depends upon bulk diffusion from grain boundaries to pores. As mentioned in section 2.1, this theoretical understanding developed along with a practical technique: Coble's strategy of preventing grains from enveloping pores allowed the first commerical applications of transparent ceramics[6].

These models, however, assume a uniform initial grain size, and a periodic arrangement of particles and voids, which limits their predictive power. More realistic microstructures can be modeled using kinetic Monte Carlo techniques. These models give plausible coarsening and densification behavior for final stage sintering, and generate plots of grain boundaries that resemble experimentally-observed microstructures, given realistic rates of grain boundary migration, surface diffusion, and diffusion from grain boundaries to pores[127, 128].

3.2 Grain boundary grooving in YAG: First and second stage sitnering

In the first two stages of sintering, as described by Coble, a single continuous void percolates through the entire sample. This void shrinks as material is transported to it from grain boundaries. The end of the second stage of sintering is marked by the closure of pores, which is expected after a shrinkage of 6% ~ 10%[8].

The work of Peters and Reimanis[129] measured the rate of material transport between grain boundaries and free surfaces which intersect those grain boundaries. This is the same condition expected during first and second stage sintering. They conclude that the controlling mechanism in grain boundary grooving of YAG is bulk diffusion of oxygen. They observed an activation energy of 330 ± 75kJ/mole for diffusion from grain boundaries to nearby surface sites, which is consistent with results from oxygen tracer studies[130]. Since Y transport does not control this process, as would be expected from its much lower bulk diffusivity rate, they conclude that Y transport during grain-boundary grooving operates by some more-rapid mechanism, such as surface diffusion.

3.3 Rare earth ion diffusion in YAG: Final stage sintering

During the final stage of sintering, pores will cease to connect distant grains, and so the available routes for diffusion are expected to be grain boundaries and grain interiors.

The diffusion of RE elements in single-crystal YAG was studied by Cherniak[131] as a stand-in for Y tracer diffusion. His results are summarized in figure 5. Diffusion activation energies were similar for all RE elements studied. La, Nd, and Yb activation energies varied systematically with ion size. For example, the diffusivity of Nd was found to be $D = 0.163 \exp\left(\frac{(-576 \pm 15) kJ/mol}{RT}\right) m^2/s$ and that of Yb was found to be $D = 0.015 \exp\left(\frac{(-540 \pm 26) kJ/mol}{RT}\right) m^2/s$, with activation energies simlar to that observed by Parthasarathy et al.[132] for Nbarro-Herring creep. Both the diffusivity that limits creep and the RE bulk diffusion rates are much lower than the measured diffusivity of oxygen, or the expected rate for aluminum. Since the ionic radii of Nd and Yb bracket that of Y, and all have similar chemical properties, Cherniak argues that Y diffusion kinetics are likely similar to those observed for RE, and that Y transport limits the rate of creep.

The similar results for the diffusion kinetics mentioned above suggest that it may be relevant to discuss work on Yb diffusion in the grain boundaries of YAG, carried out by Jimenez-Melendo, Haneda, and Nozawa[133], as a means of estimating Nd transport rates during final stage sintering. This study showed a bulk Yb diffuisivity of

$$D = 0.087 \exp\left(\frac{(-565 \pm 85)\, kJ/mol}{RT}\right) m^2/s$$

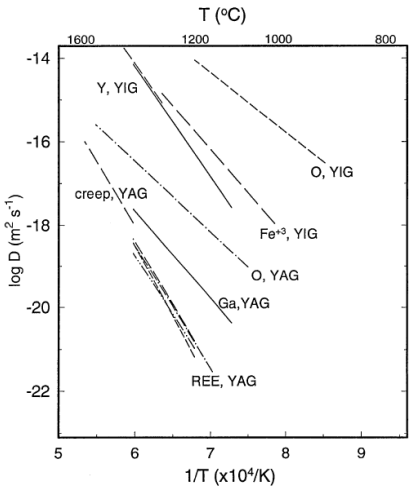

Figure 5: Diffusivity as a function of temperature for a variety of processes in YAG and YIG. Of particular interest are RE and oxygen ion diffusivities, and creep rates. From Cherniak[131].

, which is comparable to Cherniak's results, as well as a grain boundary diffuisivity of

$$D = 2100 \exp\left(\frac{(-530 \pm 190)\, kJ/mol}{RT}\right) m^2/s$$

, given an average grain size of $\approx 2\mu m$.

The results Wisdom[124] obtained when sintering waveguide structures called for investigation of diffusion in single-phase YAG, and so he constructed diffusion couples by bonding together phase-pure YAG ceramics with 1 μm grains . The results were not interpreted in terms of grain boundary diffusivity directly, but rather, in terms of κ. Given that $\kappa t^{0.3} = \exp\left(\frac{E_\Lambda}{RT} - A\right)$, diffusion couples at three temperatures in the regime of negligible grain growth gave $E_\Lambda = 314$ kJ/mol, and $A = 21.22$.

3.4 Interaction between sintering and solute diffusion

It is important to note that dopant diffusion is influenced by microstructure. Bulk diffusion will be enhanced near pores due to an excess vacancy concentration

$$\Delta C = C_0 \frac{\gamma \delta^3}{kT}\left(\frac{1}{\rho}\right)$$

, where $C_0$is the vacancy concentration under a flat surface, δ^3 is the volume of a vacancy, and ρ is the reciprocal of the sum of the reciprocals of the minimum

and maximum radius of the pore[8]. The flux of vacancies away from pores eventually causes them to close completely, ending their influence on bulk diffusion. Similarly, extended surfaces and grain boundaries within a ceramic are unstable, and their role as high-diffusivity paths decreases as they are eliminated by the action of sintering.

While the diffusion of solute ions can drive grain boundary migration, such an effect is observed much less often in bulk materials, in ceramic systems, and in dilute solutions[134]. All three of these factors suggest that the effect of a RE solute on sintering will be more subtle, and limited to the effect of local RE concentration on material properties.

Part II
Experimental Program

4 Engineering goals

The ultimate goal of this research is to create new options for laser system designers, offering them control over the placement of active species within solid-state amplifiers; a few notions of how to use this control are listed in section 2.5.2. Achieving this goal would mean developing the field of tailored ceramics to the point that a ceramic green body can be formed such that it can be sintered into a laser amplifier with the active ion distributed according to a practical design specification. This practical goal can be broken down into two parts: the more fundamental goal of understanding solute mobility during the sintering, and the process-centered goal of developing appropriate green body fabrication techniques.

4.1 Choice of a model system

Neodymium-doped yttrium aluminum garnet (Nd:YAG) is well-studied as a laser ceramic material. A wide variety of techniques for material synthesis and sintering have been published, and high-quality powders are available commercially, from several suppliers. Finally, YAG benefits from a wide and deep body of literature, allowing some predictions of dopant migration during sintering to be made based on existing data.

Predicting the movement of Nd ions over the full course of sintering, however, will require some new data on the Nd:YAG system, and would benefit from an extension of the current knowledge of Nd diffusion in partially-sintered YAG. By contrast, appropriate fabrication techniques can be developed with the benefit of a well-developed understanding of ceramics processing and its effect on transparency, but the challenge of controling dopant placement while maintaining the excellent optical properties of state-of-the-art transparent ceramics is expected to be difficult in practical terms. Fortunately, both goals can

be met within the same set of experiments, as will be described in section 6. Equally fortunately, each of these goals can be met independently of the other: an experiment that fails to illuminate the process of diffusion may result in a sample of good optical quality, and an opaque sample may yield data that can be generalized to predict the behavior of Nd in later, transparent samples.

4.2 Green body fabrication

Given an appropriate sintering method, transparent ceramic fabrication techniques tend to fail by either producing a non-uniform green body in which the larger pores fail to sinter away, by introducing impurities, or by causing errors in stoichiometry.

The goal, therefore, is to find a process which allows as much flexibility as possible in the placement of powders with different doping levels, without sacrificing purity or introducing variations in particle size or spacing. The competing requirements of very uniform particle size and morphology, and, simultaneously, a nonuniform dopant concentration, may ultimately require trade-offs.

An additional goal is to produce green bodies with curved interfaces between regions of different doping. The only methods that have been demonstrated so far have produced planar interfaces; meeting this goal would offer laser designers more flexibility, particularly for efforts to control longitudinal modes.

4.3 Nd diffusion

The relevant measurements of Nd diffusion must cover a range of sintering conditions, and explore a range of different mechanisms, in order to have any predictive value. The change in microstructure during sintering can be expected to have important effects on ion mobility. By the same token, different methods for producing transparent ceramics call for different initial conditions, which can also be expected to affect mobility. An important goal is to gain understanding that can be generalized to future fabrication methods with as little effort as possible. Finally, a new understanding of the effects of processing conditions will inform the choice of tailored ceramic fabrication techniques, and could allow work at length scales that have previously been beyond reach.

Predictions of Nd diffusion will require reliable values for surface diffusion, grain boundary diffusion, and bulk diffusion of Nd in YAG, each of which will be applied to the model in turn, as well as a reliable description of the YAG microstructure at each stage of sintering. To be as general as possible, they should be drawn from data on a wide variety of powder diameters and morphologies, which spans the range of practical transparent ceramic precursors. There should also be some effort to measure the effect of sintering additives, especially Si, on diffusivity.

It will be especially important to observe, and then predict, any change in the dominant mechanism of diffusion. For instance, the closure of pores at the end of second-stage sintering is expected to mark a transition from conditions where surface diffusion can accomplish long-range material transport, to conditions

where material must travel through grain boundaries or through the interiors of grains; determining the amount of time required to reach this transition is therefore expected to be an important part of this work.

4.3.1 Quantifying diffusion for established procedures

Vacuum sintering of YAG green bodies, formed by slip casting or cold pressing, is an established method for producing laser ceramics. An early goal in this work will be to quantify the extent of Nd diffusion during processes which have already been shown to work.

Slip casting and cold pressing produce green bodies with different levels of porosity; the former process tends to produce parts that are less dense, but more uniform. In addition, some process call for intering additives; silicon-bearing additives are commonly used for YAG. An immediate practical benefit would come from determining what changes in Nd diffusivity can be expected by the choice of green body fabrication technique and of whether or not to add Si.

4.3.2 Exploring beyond established procedures

Techniques for transparent ceramic fabrication continue to improve, and so another important goal is to develop more general knowledge, which can be applied to future techniques. For instance, data on a wide range of initial particle sizes may reveal a trend in particle size. Similarly, if green bodies from certain processes tend to achieve closed porosity sooner than others due to the details of initial pore structure, this could have a noticeable effect on surface diffusion.

4.3.3 Crafting a numerical model

Microstructural evolution, such as coarsening, changes in pore morphology, and densification, is an important part of any model of sintering. Changes in microstructure are the purpose of sintering, but it is also important to model the microstructure over time because of its influence on continued material transport. If these same conditions could be used to predict Nd transport, based on experimental data, then existing sintering models could be extended to include active species diffusion, to inform the design of green structure concentration profiles.

A major goal of this work is to provide reliable data for sintering models. The complexity of realistic green bodies, and of the interactions between sintering and rare earth diffusion, are likely to limit the predictive power of any analytical model, and so the goal is to provide parameters that would allow an accurate numerical model. In the Nd:YAG system, such a model would need new data on grain boundary diffusion and surface diffusion as a function of temperature, on the effect of Si on Nd mobility, and on any effect Nd concentration may have on sintering.

Another important goal is to produce a working model from those data. Kinetic Monte Carlo models were mentioned in section3.1, as one method capable of modeling microstructural changes. A model similar to the one used by Hassold et al.[127] shows some promise, if it can be extended to include RE ion diffusion. Such models account for time in terms of the chance for microstructural change. Since the subject of the proposed work is really the relative rates of Nd mobility and YAG mobility (i.e., how much Nd diffusion occurs during an entire sintering process), this way of handling time is well-suited to these goals. The experimental data that will be available will provide simultaneous data on microstructural change and Nd migration, which should help such a model conform to reality.

5 Outstanding problems and un-answered questions

5.1 Challenges to transparent ceramic green-body tailoring

Several techniques for producing functionally-graded ceramics are available, but not many have been adapted to meet the demands of transparent ceramics. There have been a few successes in fabricating of tailored transparent ceramic green bodies, but the field is still under development.

Diffusion in transparent ceramics has usually only been considered as the mechanism for sintering. With the advent of tailored laser ceramics, a non-uniform distribution of activator ions is becoming a desirable option, and diffusion must now be considered for its potential to re-arrange dopants in a way that degrades laser performance. Some data are available on the diffusion of rare earth (RE) elements in YAG, but more study is needed before changes in dopant concentration profile can be predicted with any confidence.

A more complete understanding of diffusion in laser ceramics would help this development along. The unexpected broadening that prevented fabrication of a working waveguide in the example form section2.5.2 illustrates the importance of planning for the diffusion of dopant ions. That effort took into account the previously-mentioned comparative study of RE diffusion in YAG[131], but did not consider mechanisms beyond bulk diffusion. The hypothesis of transient phases as channels for rapid diffusion is worth investigating, as are other rapid diffusion routes, including grain boundaries and, in the early stages of sintering, free surfaces.

5.2 Limits of current knowledge

5.2.1 Diffusion of Nd in YAG

In fact, none of the fast diffusion paths for Nd mentioned in the previous section has been studied thoroughly. Current knowledge about the diffusion kinetics of

Nd in YAG can be used to make the following tentative predictions.

Yb [133], which behaves similarly to Y and Nd in YAG monocrystals, has a grain boundary diffusivity on the order of $10^{-7} cm^2/s$ at 1700 ℃, for YAG with grains $\approx 1\mu m$. Given a sintering time of 10 hours, and the unrealistic assumption of constant grain size, this predicts a diffusion distance on the order of a few mm. While this is only a very rough estimate of Nd mobility, it suggests that this mechanism is worth studying.

Grain boundary grooving results can be used to determine a lower limit for the rate of surface diffusion of Y: since it does not limit the rate of grain boundary grooving, it must be much greater than the rate of oxygen diffusion through the bulk: $3.8 \times 10^{-14} cm^2/s$ at 1700 ℃[129]. However, direct measurements of this process are not available.

Analytical models of sintering can be used to estimate the length of time for which surface diffusion will remain a viable path. Table 1 shows one such estimate, based on the model of Kingery and Berg[126], transport rates from Peters and Reimanis[129], and a conservative assumption that pores will close after 10% linear shrinkage. Primary particle sizes were estimated using figure 6.

Table 1: Pore closure predictions for realistic diameters of YAG powder

	Temperature (℃)					
	1700	1600	1500	1400	1300	1200
Grain size (nm)	Time to pore closure (s)					
240	3	13	42	130	400	1200
46	0.02	0.1	0.3	1	3	9

5.2.2 Fabrication methods

At the time of writing, three efforts to sinter tailored green bodies have been presented: two at a conference[107] and one for a doctoral defense[124], but these experiments measured concentration profiles only in finished parts, either because a measurement was chosen which relies on the transparency of fully-sintered parts, or because the investigator was not concerned with diffusion during sintering. Concentration profiles during earlier stages of sintering have not been reported. Also, all three examples are of ceramics made by reactive sintering. Rapid diffusion in these systems is attributed by Wisdom to transient phases, but no comparable experiments have been carried out on phase-pure green bodies to test this hypothesis.

5.3 Toward a complete model

Measurements of diffusion during the first two stages of sintering, when a continuous network of pores permeates the ceramic body, will merit further study if RE atom mobility along free surfaces is found to be significantly greater than mobility along grain boundaries or through individual grains.

If earlier work on Yb diffusion through YAG grain boundaries[133] can be taken in lieu of measurements of Nd, grain boundaries may have been the route for the observed behavior: during sintering at 1700 ℃ for 20 hours, a diffusion on the order of 1mm would be expected. Surface diffusion is another possible explanation. The early stages of sintering allow diffusion along a free surface, which is expected to be a rapid process based on grain boundary grooving experiments. Without any comparison between diffusion rates in the presence and absence of open porosity, there is no way to answer this question directly.

If the analytical model used in section 5.2.1 applies, then surface diffusion will be active for a negligible time: pore closure would occur even before the sample reached the sintering temperature. However, this model assumes a regular spacing of initial particles; larger-diameter voids could stay open longer. Given the sensitivity of this process to both length scale and temperature, as illustrated in Table 1, surface diffusion may be an important mechanism for those samples at the extremes of large initial particle size, non-uniform pore structure, low initial density, low sintering temperature, and short sintering time.

6 Finding answers

Diffusivity can be measured by fabricating diffusion couples, sintering them for a variety of times and temperatures, and then measuring the resulting concentration profiles. The expected sensitivity of this system to initial particle size and green body morphology recommends that such an experiment include a wide variety of powder sizes and green body fabrication techniques.

6.1 Obtaining powders

A wide variety of powders will be used in diffusion couples, including commercially available materials and oxides synthesized in-house.

Shin-Etsu offers a co-precipitated YAG powder with approximately 200nm diameter, which has been slip-cast and sintered into highly-transparent ceramics at LLNL. Nd-doped powder is not available from this supplier, and so a mixed nitrate process has been developed to incorporate Nd into the material. Neodymium nitrate (Rare Earth Products Ltd., A. R.) and aluminum nitrates (Aldrich, 98+%) were dissolved in deionized water, with a ratio of three Nd^{3+} ions for every five Al^{3+}. This solution was then added to YAG powder (Shin-Etsu lot RYAG-OCX-076), dried, and calcined to produce a mixed oxide. X-ray diffraction of the resulting powder showed no impurity phases after calcination at 1650 ℃, but some perovskite peaks when calcined to only 1000 ℃. Powders doped using this nitrate technique have been sintered to transparency. For diffusion couple studies, pure YAG powder with the same particle size and morphology will be obtained by carrying out a similar nitrate process, using Y in place of Nd.

Nanocerox uses flame-spray pyrolysis to produce YAG powder with a diameter of approximately 50 nm. Powder from this supplier, doped with 0.6% Nd (Y

site basis) and a proprietary Si-derived sintering aid, has been cold-pressed and vacuum sintered at LLNL to produce working laser amplifiers. This supplier has agreed to provide powder with and without the sintering aid, both with and without an optical doping of 1% Nd.

LLNL is also developing three co-precipitation synthesis methods for producing YAG powder. One of these is being adapted from earlier, un-published work on spinel. The other two methods are based on published procedures for urea precipitation[135] and carbonate precipitation[97].

6.2 Producing green bodies

The parts sintered will include green bodies formed by a mix of well-developed and novel techniques. As an experiment in diffusion, this will give the results wider applicability to future ceramic technology by including a variety of morphologies. The field of transparent ceramics tends to be circumscribed by entrenched practices until a radical advance disrupts the status quo, making wide applicability of this kind relatively scarce. As an experiment in green body fabrication, it will offer the leeway to explore several promising techniques, with samples fabricated via established techniques serving as a control. And even those parts which are not sintered to transparency will produce valuable information about Nd diffusion.

Diffusion couples will be fabricated in several morphologies. The first morphology to be studied will be a cylinder with a plane boundary parallel to its flat faces. This morphology is straightforward to produce by either cold pressing or slip casting. The second will be a cylinder with a tube-shaped boundary that is, ideally, a constant distance from the curved walls of the cylinder. This latter morphology will more closely approximate a useful graded ceramic, and the fact that the boundary will be perpendicular to the flat, polished surfaces will simplify optical measurements of doping in finished samples. Lastly, I hope to create pseudo-plane-source samples using neodymium-aluminum garnet powder, in hopes of testing Jeffrey Wisdom's hypothesis about diffusion in secondary phases.

6.2.1 Established techniques

Slip casting is an established ceramic fabrication technique which has been successfully applied to transparent ceramic fabrication[2, 136]. A gypsum mold is filled with a slurry of ceramic particles in water (slip). These particles remain in the mold as the water is drawn into the gypsum, creating a green body with a continuous, percolating pore structure, as shown in figure 6 a).

Uniaxial cold pressing is also an established fabrication technique, in which loose powder is loaded into a die, and pressure is applied with punches to consolidate the material. Because gas can become trapped in the green body as the powder is compressed, cold pressing for transparent ceramics is sometimes carried out in a vacuum environment. A typical cold-pressed green body is shown in figure 6 b).

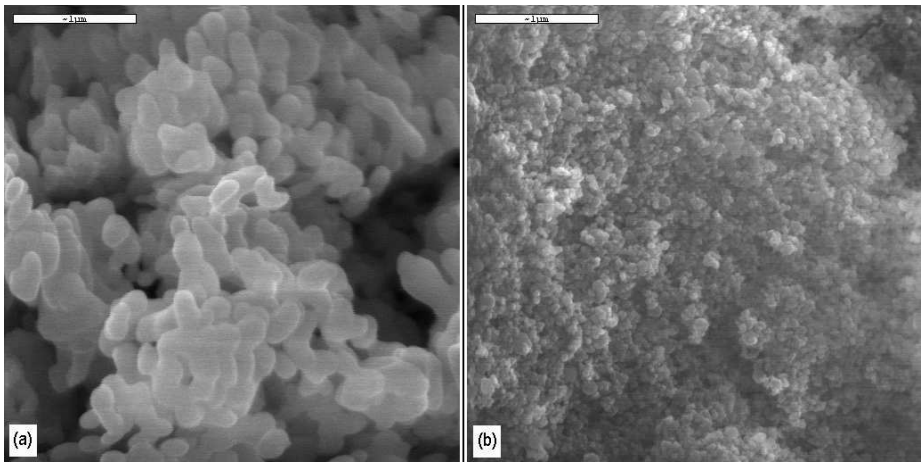

Figure 6: SEM images of ceramic green bodies. a) Slip cast Shin Etsu YAG (lot RYAG-OCX-076), showing large pores and particles roughly 240 nm in diameter. b) Cold pressed Nanocerox 0.6% Nd:YAG (lot 2LN290A), showing close packing and particles roughly 46 nm in diameter.

These techniques have been used by the author to produce transparent structures with a uniform dopant concentration, and are the most likely to produce transparent ceramics from green bodies with non-uniform Nd concentration.

6.2.2 Novel techniques

In the same vein as Messing's report of tape casting, green body fabrication techniques will be employed which are new to transparent ceramics work.

Following earlier work within the group, I am revisiting the use of poly(ethylene glycol) (PEG) as a binder, and at the same time beginning work on polystyrene (PS). The intent with these binders is to dissolve the polymer in a solvent, and produce a formable mixture that is approximately 3/8 ceramic powder, 3/8 polymer, and 1/4 solvent, by volume. The binders under study are both soluble in n-methylpyrrolidinone (NMP), which has a moderately low vapor pressure allowing ample time to form green bodies before the mixture hardens by evaporation. PEG has also been tested with both water and isopropyl alcohol as solvents. The resulting mixtures can be formed with gloved hands, similar to plastecine clay. Mixing and degassing were accomplished using a Thinky AR-250 centrifugal mixer.

In addition to working the material by hand, several other ceramic techniques will be applied. Extrusion of mixtures like the ones discussed above will be attempted using graphite dies. Previous attempts at extrusion resulted in translucent samples, which was attributed to second-phase oxides, reaction products of aluminum from die walls; contamination from graphite dies, by contrast, would burn away along with the polymer. Thinner mixtures, with more

solvent and perhaps less binder, will be formed by such methods as tape casting, and casting onto the walls of a rotating container.

Both kinds of binder have been found to burn out completely by firing green bodies at 1000 ℃ in air, and vacuum sintering has produced translucent parts with opaque regions. The full program of de-agglomeration and classification procedures was not performed on the powder for these samples, and implementing such procedures is expected to reduce the level of porosity in finished parts.

In addition to working the material with gloved hands, several other ceramic techniques will be applied. Extrusion of mixtures like the ones discussed above will be attempted using graphite dies. Previous attempts at extrusion resulted in translucent samples, which was attributed to second-phase oxides, reaction products of aluminum from die walls; contamination from graphite dies, by contrast, would burn away along with the polymer. Thinner mixtures, with more solvent and perhaps less binder, will be formed by such methods as tape casting, and casting onto the walls of a rotating mold.

Diffusion couples will be fabricated in several morphologies. The first morphology to be studied will be a cylinder with a plane boundary parallel to its flat faces. This morphology is straightforward to produce by either cold pressing or slip casting. If early diffusion results are promising, a waveguide structure will be attempted, using a thin layer of doped material sandwiched between undoped material. Novel fabrication techniques will be used to produce another shape of diffusion couple, a cylinder with a tube-shaped boundary that is, ideally, a constant distance from the curved walls of the cylinder. This latter morphology will more closely approximate a useful graded ceramic, and the fact that the boundary will be perpendicular to the flat, polished surfaces will simplify optical measurements of doping in finished samples.

6.3 Sintering samples

Several duplicates of each morphology will be fabricated. One of each will be chosen at random and sintered according to established time and temperature profiles for transparent YAG. The remaining green bodies will be cleaved, allowing multiple arrested sintering experiments to be run with each. SEM and EDS examination of a representative sample will determine green body microstructure and initial doping profile.

Cleaved samples will then be systematically assigned to sintering times and temperatures, so that a mix of fabrication techniques and doping profiles are represented at each temperature. The samples will then be sintered in no particular order, according to a randomly generated set of numbers.

6.4 Measuring microstructure

Sintered samples will be ground and polished to allow SEM observation. At this point, EDS measurements will determine the extent of diffusion in each sample. In fully-sintered samples, optical microscopy may be appropriate,

and thermal etching of the surface may be necessary in order to reveal grain structure. It may also be possible to collaborate with Stanford to use their apparatus for stimulated-emission measurements of Nd concentration.

Stereology will be used to ensure meaningful and statistically significant measurements of grain size and surface area.

6.5 Measuring concentration

While examining sintered parts with an SEM, a rough Nd profile can be obtained using energy dispersive spectrometry. Preliminary results suggest that EDS will not be sufficiently sensitive to detect the low Nd concentrations far from the diffusion couple, and so more detailed profiles will be measured by SIMS, or by optical fluorescence.

6.6 Interpreting diffusion results

6.6.1 Diffusivity

Concentration profiles measured will resemble those obtained by Jimenez-Melendo, Haneda, and Nozawa[133], with a form that reflects the influence of bulk diffusion at low distances from the diffusion couple, transitioning to a form that reflects fast diffusion at larger distances. The concentration profile expected due to surface diffusion is similar to the profile expected due to grain boundary diffusion, with a functional dependence on distance of $\exp\left(x^{6/5}/b\right)$. In cases where three mechanisms are active, it is often possible to measure all three on a single curve[137].

6.6.2 Mechanism change

Diffusion profiles obtained before and after pore closure will be used to differentiate between surface and grain boundary diffusion. If surface diffusion is found to be the dominant mechanism, then profiles will change very slowly after pores close.

If the analytical models used in

7 Solving problems

In parallel with the effort to answer basic questions about diffusion, this work intends to produce results of practical value, as well. After the initial run of diffusion couples has been sintered, the various processing techniques can be evaluated based on the quality of samples produced. Samples will be polished, and their optical properties characterized. Some methods can be abandoned, and the processes that remain can be improved, with the goal of obtaining laser-quality parts.

7.1 Optical characterization

A Perkin-Elmer Lambda 9 UV-VIS-NIR spectrophotometer is used for preliminary characterization of transparent samples. Absorption peaks are useful for estimating the average optical doping of the sample, and would reveal any contamination by colored ions. A broad reduction in transmission that is almost independent of wavelength indicates scattering; however, bulk scattering that does not exceed a few percent can escape notice due to surface reflections and surface scattering.

Figure 7 shows optical transmission curves for some transparent ceramic samples fabricated at LLNL. SCSE 70 and 71 are un-doped samples, from slip-cast green bodies made with precipitated powder, similar to the one shown in figure 6 a). JDK-III-93 A and B are 0.6% Nd:YAG samples from cold-pressed green bodies made with FSP powder, similar to the oneshown in figure 6 b).

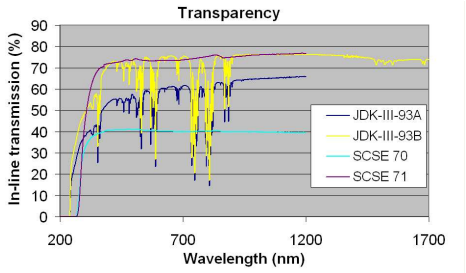

Figure 7: In-line transmission curves of 0.6% Nd:YAG cold-pressed samples after vacuum sintering and HIP, and 1% Nd:YAG single crystal.

7.2 Laser testing

The most transparent samples are placed in a laser cavity, at the Brewster angle, and pumped with 808nm laser diode light. The threshold pump power for oscillation and the slope efficiency of a sample is measured for each of several different output couplers. These data are used as a very sensitive measurement of losses. An example is shown in figure 8. With an 80% output coupler, the slope efficiency is the same for all three samples. Iin a cavity with a 95% output coupler, the scattering of these ceramic samples shows itself as a lower slope efficiency, because laser light passes through the amplifier more times before exiting the cavity, and has more opportunities to scatter.

7.3 Numerical modeling

Molecular dynamics (MD) simulations are being developed by George Gilmer. Currently, he is working on the relatively simple structure of Y_2O_3, doing three-particle sintering simulations that should offer insight into the mechanisms of

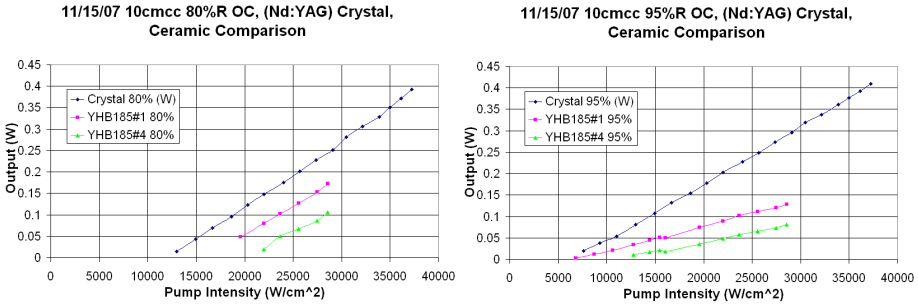

Figure 8: Laser output power versus optical pumping power for laser ceramic samples produced at LLNL.

sintering for nanometer-scale powders. The results of such simulations will also contain predictions for surface and grain-boundary diffusivity.

MD will also be useful in predicting the jump frequency for ions in several different situations within the bulk, for use in analytical first-principles calculations of diffusivity.

Kinetic Monte Carlo simulations will also be carried out, using experimental rates of diffusion and grain growth to model changes in microstructure and Nd^{3+} ion diffusion.

References

[1] A. Ikesue, Y. L. Aung, T. Taira, T. Kamimura, K. Yoshida, and G. L. Messing, "Progress in ceramic lasers," *Annual Review of Materials Research*, vol. 36, pp. 397–429, 2006.

[2] A. Kaminskii, M. Akchurin, V. Alshits, K. Ueda, K. Takaichi, J. Lu, T. Uematsu, M. Musha, A. Shirikawa, V. Gabler, H. Eichler, H. Yagi, T. Yanagitani, S. Bagayev, J. Fernandez, and R. Balda, "New data on the physical properties of y3al5o12-based nanocrystalline laser ceramics," *Crystallography Reports*, vol. 48, pp. 515–519, May 2003.

[3] Ikesue, A., Aung, and Y. Lin, "Synthesis and performance of advanced ceramic lasers," *Journal of the American Ceramic Society*, vol. 89, pp. 1936–1944, June 2006.

[4] R. R. Monchamp, "The distribution coefficient on neodymium and lutetium in czochralski grown y3al5o12," *Journal of Crystal Growth*, vol. 11, pp. 310–312, December 1971.

[5] J. D. Kuntz, J. P. Hollingsworth, and T. F. Soules, "Transparent ceramics for lasers," *Journal of the American Ceramic Society*, 2008. in press.

[6] R. L. Coble, "Transparent alumina and method of preparation," March 1962.

[7] R. L. Coble, "Sintering crystalline solids. ii. experimental test of diffusion models in powder compacts," *Journal of Applied Physics*, vol. 32, no. 5, pp. 793–799, 1961.

[8] R. L. Coble, "Initial sintering of alumina and hematite," *Journal of the American Ceramic Society Journal of the American Ceramic Society*, vol. 41, pp. 55–62, February 1958.

[9] J. E. Burke, "Role of grain boundaries in sintering.," *Journal of the American Ceramic Society*, vol. 40, no. 3, pp. 80–85, 1957.

[10] R. L. Coble, "Sintering crystalline solids. i. intermediate and final state diffusion models," *Journal of Applied Physics*, vol. 32, no. 5, pp. 787–792, 1961.

[11] J. G. Peelen, *Alumina: Sintering and optical properties*. PhD thesis, Technische Hogeschool Eindhoven, Eindhoven, May 1977.

[12] T. F. Soules, "Light transmission through a lucalox plate," tech. rep., General Electric, 1972.

[13] J. G. J. Peelen and R. Metselaar, "Light scattering by pores in polycrystalline materials: Transmission properties of alumina," *Journal of Applied Physics*, vol. 45, no. 1, pp. 216–220, 1974.

[14] E. Carnall, S. E. Hatch, L. S. Ladd, and W. F. Parsons, "Method of molding magnesium fluoride," December 1966.

[15] S. E. Hatch and R. J. Weagley, "Calcium fluoride optical elements and method for making same," December 1967.

[16] E. Carnall, "Lanthanum fluoride infrared trans-mitting optical elements," September 1961.

[17] E. Carnall and L. S. Ladd, "Process of hot pressing magnesium oxide infrared transmitting opti-cal elements," *United States Patent*, vol. 3131026, April 1964.

[18] E. Carnall and S. E. Hatch, "Process of hot pressing magnesium oxide infrared transmitting optical elements," *United States Patent*, vol. 3402226, December 1968.

[19] E. Carnall and D. W. Roy, "Method of forming zinc oxide infrared transmitting optical element," *United States Patent*, vol. 3416907, December 1968.

[20] E. Carnall, P. B. Mauser, W. F. Parsons, D. W. Roy, and E. Kodak, "Process for molding zinc sulfide," *United States Patent*, vol. 3131238, April 1964.

[21] W. F. Parsons, "Optical materials research," *Appl. Opt.*, vol. 11, pp. 43+, January 1972.

[22] L. A. Brisette, P. L. Burnett, R. M. Spriggs, and T. Vasilos, "Thermomechanically deformed y2o3," *Journal of the American Ceramic Society*, vol. 49, no. 3, pp. 165–166, 1966.

[23] R. A. Lefever and J. Matsko, "Transparent yttrium oxide ceramics," *Materials Research Bulletin*, vol. 2, pp. 865–869, September 1967.

[24] S. K. Dutta and G. E. Gazza, "Transparent y2o3 by hot-pressing," *Materials Research Bulletin*, vol. 4, pp. 791–796, November 1969.

[25] R. C. Anderson, "Transparent yttria-based ceramics and method for producing same," December 1970.

[26] R. C. Anderson, "Transparent zirconia, hafnia-, and thoria-rare earth ceramics," February 1972.

[27] S. E. Hatch, W. F. Parsons, and R. J. Weagley, "Hot-pressed polycrystalline caf[sub 2]:dy[sup 2 +] laser," *Applied Physics Letters*, vol. 5, no. 8, pp. 153–154, 1964.

[28] C. Greskovich and J. P. Chernoch, "Polycrystalline ceramic lasers," *Journal of Applied Physics*, vol. 44, no. 10, pp. 4599–4606, 1973.

[29] C. D. Greskovich and W. L. Roth, "Polycrystalline ceramic lasers," July 1975.

[30] C. Greskovich and K. N. Woods, "Fabrication of transparent tho2-doped y2o3," *Ceramic Bulletin*, vol. 52, no. 5, pp. 473–478, 1973.

[31] C. Greskovich and J. P. Chernoch, "Improved polycrystalline ceramic lasers," *Journal of Applied Physics*, vol. 45, no. 10, pp. 4495–4502, 1974.

[32] G. Toda and I. Matsuyama, "Effect of beo addition on sintering of transparent y2o3," *Journal of the Japan Society of Powder and Powder Metallurgy*, vol. 35, pp. 486–491, 1988.

[33] W. H. Rhodes and J. F. Reid, "Transparent yttria ceramics containing magnesia or magnesium aluminate," November 1979.

[34] W. H. Rhodes, "Transparent yttria ceramics and method for producing same," *United States patent*, vol. 4147744, April 1979.

[35] W. H. Rhodes, "Controlled transient solid second-phase sintering of yttria," *Journal of the American Ceramic Society*, vol. 64, no. 1, pp. 13–19, 1981.

[36] K. Majima, N. Niimi, M. Watanabe, S. Katsuyama, and H. Nagai, "Effect of lif addition on the preparation and transparency of vacuum hot pressed y2o3," *Materials Transactions*, vol. 35, no. 9, pp. 645–650, 1994.

[37] J. W. Mccauley and N. D. Corbin, "Phase relations and reaction sintering of transparent cubic aluminum oxynitride spinel (alon)," *Journal of the American Ceramic Society*, vol. 62, no. 9-10, pp. 476–479, 1979.

[38] R. L. Gentilman, E. A. Maguire, and L. E. Dolhert, "Transparent aluminum oxynitride and method of manufacture," May 1985.

[39] R. J. Bratton, "Translucent sintered mgal2o4," *Journal of the American Ceramic Society*, vol. 57, no. 7, pp. 283–286, 1974.

[40] D. Roy, "Hot-pressed mgal2o4 for ultraviolet (uv), visible, and infrared (ir) optical requirements," in *Emerging Optical Materials* (S. Musikant, ed.), vol. 297, pp. 13+, Society of Photo-optical Instrumentation Engineers, January 1981.

[41] D. W. Roy and F. J. Stermole, "Method for manufacturing a transparent ceramic body," August 1976.

[42] G. R. Villalobos, J. S. Sanghera, and I. D. Aggarwal, "Degradation of magnesium aluminum spinel by lithium fluoride sintering aid," *Journal of the American Ceramic Society*, vol. 88, no. 5, pp. 1321–1322, 2005.

[43] J.-G. Li, T. Ikegami, J.-H. Lee, and T. Mori, "Low-temperature fabrication of transparent yttrium aluminum garnet (yag) ceramics without additives," *Journal of the American Ceramic Society*, vol. 83, no. 4, pp. 961–963, 2000.

[44] M. Shimada, T. Endo, T. Saito, and T. Sato, "Fabrication of transparent spinel polycrystalline materials," *Materials Letters*, vol. 28, pp. 413–415, October 1996.

[45] K. Tsukuma, "Transparent mgal2o4 spinel ceramics produced by hip post-sintering," *Nippon Seramikkusu Kyokai gakujutsu ronbunshi (Journal of the Ceramic Society of Japan)*, vol. 114, pp. 802–806, October 2006.

[46] C. R. Bickmore, K. F. Waldner, D. R. Treadwell, and R. M. Laine, "Ultrafine spinel powders by flame spray pyrolysis of a magnesium aluminum double alkoxide," *Journal of the American Ceramic Society*, vol. 79, no. 5, pp. 1419–1423, 1996.

[47] X. H. Chang, T. C. Lu, Y. Zhang, X. J. Lu, Q. Liu, C. B. Huang, J. Q. Qi, M. Y. Lei, C. X. Huang, and L. B. Lin, "Mgal2o4 transparent nanoceramics prepared by sintering under ultrahigh pressure," vol. 280-283, pp. 549–552, 2005.

[48] T. Hartnett, M. Greenberg, and R. L. Gentilman, "Optically transparent yttrium oxide," August 1988.

[49] B. P. Borglum, "Method of producing optically transparent yttrium oxide," April 1991.

[50] A. Fujii and K. Shibata, "Light transmitting yttria sintered body and its preparation," December 1991.

[51] Belyakov, A., Lemeshev, D., Lukin, E., Valnin, G., Grinberg, and E., "Optically transparent ceramics based on yttrium oxide using carbonate and alkoxy precursors," *Glass and Ceramics*, vol. 63, pp. 262–264, July 2006.

[52] T. Stefanik, R. Gentilman, and P. Hogan, "Nano-composite optical ceramics for infrared windows and domes," in *Window and Dome Technologies and Materials X* (R. W. Tustison, ed.), vol. 6545A of *Proceedings of SPIE*, (Bellinghamton, WA), May 2007.

[53] M. Mitomo, Y. Moriyoshi, T. Sakai, T. Ohsaka, and M. Kobayashi, "Translucent beta-sialon ceramics," *Journal of Materials Science Letters*, vol. 1, pp. 25–26, January 1982.

[54] M.-A. Einarsrud and M. Mitomo, "Mechanism of grain growth of beta-sialon," *Journal of the American Ceramic Society*, vol. 76, no. 6, pp. 1624–1626, 1993.

[55] Z. Shen, M. Nygrenm, and U. Halenius, "Absorption spectra of rare-earth-doped alpha-sialon ceramics," *Journal of Materials Science Letters*, vol. 16, February 1997.

[56] X. Su, P. Wang, W. Chen, Y. Cheng, and D. Yan, "Effect of processing on microstructure and optical properties of dy-alpha-sialon," *Materials Letters*, vol. 58, pp. 3340–3344, October 2004.

[57] M. I. Jones, H. Hyuga, K. Hirao, and Y. Yamauchi, "Highly transparent lu-alpha-sialon," *Journal of the American Ceramic Society*, vol. 87, no. 4, pp. 714–716, 2004.

[58] J. Xue, Q. Liu, and L. Gui, "Lower-temperature hot-pressed dy-alpha-sialon ceramics with an lif additive," *Journal of the American Ceramic Society*, vol. 90, pp. 1623–1625, May 2007.

[59] D. Clay, D. Poslusny, M. Flinders, S. D. Jacobs, and R. A. Cutler, "Effect of lial5o8 additions on the sintering and optical transparency of lialon," *Journal of the European Ceramic Society*, vol. 26, no. 8, pp. 1351–1362, 2006.

[60] A. Granon, P. Goeuriot, and F. Thevenot, "Aluminum magnesium oxynitride: A new transparent spinel ceramic," *Journal of the European Ceramic Society*, vol. 15, no. 3, pp. 249–254, 1995.

[61] A. Pechenik, G. J. Piermarini, and S. C. Danforth, "Fabrication of transparent silicon nitride from nanosize particles," *Journal of the American Ceramic Society*, vol. 75, no. 12, pp. 3283–3288, 1992.

[62] R.-J. Sung, T. Kusunose, T. Nakayama, Y.-H. Kim, T. Sekino, S. Lee, and K. Niihara, "Mechanical properties of transparent polycrystalline silicon nitride," vol. 317-318, pp. 305–308, Trans Tech Publications, 2006.

[63] Y. Xiong, Z. Fu, Y. Wang, and F. Quan, "Fabrication of transparent aln ceramics," *Journal of Materials Science*, vol. 41, pp. 2537–2539, April 2006.

[64] N. Kuramoto and H. Taniguchi, "Transparent aln ceramics," *Journal of Materials Science Letters*, vol. 3, pp. 471–474, June 1984.

[65] N. Kuramoto, H. Taniguchi, and I. Aso, "Translucent aln ceramic substrate," *Components, Hybrids, and Manufacturing Technology, IEEE Transactions on [see also IEEE Trans. on Components, Packaging, and Manufacturing Technology, Part A, B, C]*, vol. 9, no. 4, pp. 386–390, 1986.

[66] N. Kuramoto, H. Taniguchi, and I. Aso, "Development of translucent aluminum nitride ceramics," *American Ceramic Society Bulletin*, vol. 68, no. 4, pp. 883–887, 1989.

[67] C. D. Greskovich, D. A. Cusano, and F. A. Dibianca, "Preparation of yttria-gadolinia ceramic scintillators by vacuum hot pressing," *United States Patent*, vol. 4466929, August 1984.

[68] J. Leppert, "Method for producing rare earth oxysulfide powder," October 2001.

[69] D. A. Cusano, C. D. Greskovich, and F. A. Dibianca, "Rare-earth-doped yttria-gadolina ceramic scintillators," May 1988.

[70] S. L. Dole and C. D. Greskovich, "Method of forming yttria-gadolinia ceramic scintillator from ammonium dispersed oxalate precipitates," March 1992.

[71] A. Lempicki, C. Brecher, P. Szupryczynski, H. Lingertat, V. V. Nagarkar, S. V. Tipnis, and S. R. Miller, "A new lutetia-based ceramic scintillator for x-ray imaging," *Nuclear Instruments and Methods in Physics Research Section A: Accelerators, Spectrometers, Detectors and Associated Equipment*, vol. 488, pp. 579–590, August 2002.

[72] N. Matsuda, M. Tamatani, and K. Yokota, "Method of manufacturing a rare earth oxysulfide ceramic," June 1988.

[73] C. D. Greskovich, W. P. Minnear, C. R. O'Clair, E. O. Gurmen, and R. J. Riedner, "Transparent polycrystalline garnets," January 1996.

[74] A. Lempicki, C. Brecher, H. Lingertat, and V. K. Sarin, "High-density polycrystalline lutetium silicate materials activated with ce," November 2005.

[75] Y.-K. Liao, D.-Y. Jiang, and J.-L. Shi, "Transparent lutetium aluminum garnet sintered from carbonate coprecipitated powders," *Materials Letters*, vol. 59, pp. 3724–3727, December 2005.

[76] H.-L. Li, X.-J. Liu, and L.-P. Huang, "Fabrication of transparent cerium-doped lutetium aluminum garnet (luag:ce) ceramics by a solid-state reaction method," *Journal of the American Ceramic Society*, vol. 88, no. 11, pp. 3226–3228, 2005.

[77] J. D. Kuntz, J. J. Roberts, M. Hough, and N. J. Cherepy, "Multiple synthesis routes to transparent ceramic lutetium aluminum garnet," *Scripta Materialia*, vol. 57, pp. 960–963, November 2007.

[78] C. E. Land and P. D. Thacher, "Ferroelectric ceramic electrooptic materials and devices," *Proceedings of the IEEE*, vol. 57, no. 5, pp. 751–768, 1969.

[79] G. H. Haertling and C. E. Land, "Hot-pressed (pb,la)(zr,ti)o3 ferroelectric ceramics for electrooptic applications," *Journal of the American Ceramic Society*, vol. 54, no. 1, pp. 1–11, 1971.

[80] G. H. Haertling, "Improved hot-pressed electrooptic ceramics in the (pb,la)(zr,ti)o3 system," *Journal of the American Ceramic Society*, vol. 54, no. 6, pp. 303–309, 1971.

[81] G. Haertling and C. Land, "Recent improvements in the optical and electrooptic properties of plzt ceramics," *Ferroelectrics*, vol. 3, pp. 269–280, 1972.

[82] G. S. Snow, "Improvements in atmosphere sintering of transparent plzt ceramics," *Journal of the American Ceramic Society*, vol. 56, no. 9, pp. 479–480, 1973.

[83] K. K. Li and Q. Wang, "Electro-optic ceramic material and device," June 2004.

[84] H. Jiang, Y. K. Zou, Q. Chen, K. K. Li, R. Zhang, Y. Wang, H. Ming, and Z. Zheng, "Transparent electro-optic ceramics and devices," in *Optoelectronic Devices and Integration. Edited by Ming, Hai; Zhang, Xuping; Chen, Maggie Yihong. Proceedings of the SPIE, Volume 5644, pp. 380-394 (2005).* (H. Ming, X. Zhang, and M. Y. Chen, eds.), vol. 5644 of *Presented at the Society of Photo-Optical Instrumentation Engineers (SPIE) Conference*, pp. 380–394, January 2005.

[85] A. S. S. de Camargo, Luiz, I. A. Santos, D. Garcia, and J. A. Eiras, "Structural and spectroscopic properties of rare-earth (nd[sup 3+], er[sup 3+], and yb[sup 3+]) doped transparent lead lanthanum zirconate titanate ceramics," *Journal of Applied Physics*, vol. 95, no. 4, pp. 2135–2140, 2004.

[86] A. S. S. de Camargo, E. R. Botero, D. Garcia, J. A. Eiras, and L. A. O. Nunes, "Nd[sup 3+]-doped lead lanthanum zirconate titanate transparent ferroelectric ceramic as a laser material: Energy transfer and stimulated emission," *Applied Physics Letters*, vol. 86, no. 15, pp. 152905–152907, 2005.

[87] G. de With and H. J. A. van Dijk, "Translucent y3al5o12 ceramics," *Materials Research Bulletin*, vol. 19, pp. 1669–1674, December 1984.

[88] A. Ikesue, T. Kinoshita, K. Kamata, and K. Yoshida, "Fabrication and optical properties of high-performance polycrystalline nd:yag ceramics for solid-state lasers," *Journal of the American Ceramic Society*, vol. 78, no. 4, pp. 1033–1040, 1995.

[89] A. Ikesue, K. Kamata, and K. Yoshida, "Synthesis of nd3+,cr3+-codoped yag ceramics for high-efficiency solid-state lasers," *Journal of the American Ceramic Society*, vol. 78, no. 9, pp. 2545–2547, 1995.

[90] K.-I. Ueda, "Advances in ceramic laser media," in *Frontiers in Optics*, Laser Science XXIII, (Vancouver, BC, Canada), 2007.

[91] A. Ikesue and K. Yoshida, "Scattering in polycrystalline nd:yag lasers," *Journal of the American Ceramic Society*, vol. 81, no. 8, pp. 2194–2196, 1998.

[92] A. Ikesue and K. Kamata, "Microstructure and optical properties of hot isostatically pressed nd:yag ceramics," *Journal of the American Ceramic Society*, vol. 79, no. 7, pp. 1927–1933, 1996.

[93] A. Ikesue, K. Kamata, and K. Yoshida, "Effects of neodymium concentration on optical characteristics of polycrystalline nd:yag laser materials," *Journal of the American Ceramic Society*, vol. 79, no. 7, pp. 1921–1926, 1996.

[94] V. Lupei, A. Lupei, S. Georgescu, T. Taira, Y. Sato, and A. Ikesue, "The effect of nd concentration on the spectroscopic and emission decay properties of highly doped nd:yag ceramics," *Physical Review B*, vol. 64, no. 9, pp. 092102–092105, 2001.

[95] V. Lupei, A. Lupei, N. Pavel, T. Taira, I. Shoji, and A. Ikesue, "Laser emission under resonant pump in the emitting level of concentrated nd:yag ceramics," *Applied Physics Letters*, vol. 79, no. 5, pp. 590–592, 2001.

[96] M. Sekita, H. Haneda, T. Yanagitani, and S. Shirasaki, "Induced emission cross section of nd:y[sub 3]al[sub 5]o[sub 12] ceramics," *Journal of Applied Physics*, vol. 67, pp. 453–458, January 1990.

[97] J.-G. Li, T. Ikegami, J.-H. Lee, T. Mori, and Y. Yajima, "Co-precipitation synthesis and sintering of yttrium aluminum garnet (yag) powders: the effect of precipitant," *Journal of the European Ceramic Society*, vol. 20, pp. 2395–2405, December 2000.

[98] J. Lu, M. Prabhu, J. Song, C. Li, J. Xu, K. Ueda, A. A. Kaminskii, H. Yagi, and T. Yanagitani, "Optical properties and highly efficient laser oscillation of nd:yag ceramics," *Applied Physics B: Lasers and Optics*, vol. 71, pp. 469–473, October 2000.

[99] J. Lu, M. Prabhu, J. Song, C. Li, J. Xu, K. I. Ueda, A. A. Kaminskii, H. Yagi, and T. Yanagitani, "Production of yttrium aluminum garnet fine powder (ittoriumu aruminiumu ganetto bifuntai no seizohoho," 1998.

[100] J. Lu, M. Prabhu, J. Song, C. Li, J. Xu, K. I. Ueda, A. A. Kaminskii, H. Yagi, and T. Yanagitani, "Production of yttrium aluminum garnet powder (ittoriumu aruminumu ganetto funmatsu no seizohoho)," 1998.

[101] J. Lu, T. Murai, K. Takaichi, T. Uematsu, K. Misawa, M. Prabhu, J. Xu, K. Ueda, H. Yagi, T. Yanagitani, A. A. Kaminskii, and A. Kudryashov, "72 w nd:y[sub 3]al[sub 5]o[sub 12] ceramic laser," *Applied Physics Letters*, vol. 78, no. 23, pp. 3586–3588, 2001.

[102] Y. Qi, X. Zhu, Q. Lou, J. Ji, J. Dong, and Y. Wei, "Nd:yag ceramic laser obtained high slope-efficiency of 62% in high power applications," *Optics Express*, vol. 13, pp. 8725–8729, October 2005.

[103] J. Lu, K.-I. Ueda, H. Yagi, T. Yanagitani, Y. Akiyama, and A. A. Kaminskii, "Neodymium doped yttrium aluminum garnet (y3al5o12) nanocrystalline ceramics–a new generation of solid state laser and optical materials," *Journal of Alloys and Compounds*, vol. 341, pp. 220–225, July 2002.

[104] K.-I. Ueda, "verbal communication," 2005.

[105] Y. Sato, T. Taira, and A. Ikesue, "Spectral parameters of nd3+-ion in the polycrystalline solid-solution composed of y3al5o12 and y3sc2al3o12," *Japan Journal of Applied Physics*, vol. 42, pp. 5071–5074, August 2003.

[106] Y. Sato, I. Shoji, A. Ikesue, T. Taira, and J. Zayhowski, "The spectroscopic properties and laser characteristics of polycrystalline nd:y3scxal(5-x)o12 laser media," vol. 83 of *OSA Trends in Optics and Photonics*, pp. 444+, Optical Society of America, February 2003.

[107] "Untitled," in *3rd Laser Ceramic Symposium*, (Paris, France), October 2007.

[108] T. Ikegami, T. Mori, and Y. Yajima, "Fabrication of transparent ceramics through the synthesis of yttrium hydroxide at low temperature and doping by sulfate ions," *Journal of the ceramic Society of Japan*, vol. 107, no. 1243, pp. 297–299, 1999.

[109] A. Fukabori, M. Sekita, T. Ikegami, N. Iyi, T. Komatsu, M. Kawamura, and M. Suzuki, "Induced emission cross section of a possible laser line in nd:y[sub 2]o[sub 3] ceramics at 1.095 mu m," *Journal of Applied Physics*, vol. 101, no. 4, 2007.

[110] J. Lu, J. Lu, T. Murai, K. Takaichi, T. Uematsu, K.-I. Ueda, H. Yagi, T. Yanagitani, and A. A. Kaminskii, "Nd3+:y2o3 ceramic laser," *Japan Journal of Applied Physics*, vol. 40, pp. L1277–L1279, December 2001.

[111] J. Lu, K. Takaichi, T. Uematsu, A. Shirakawa, M. Musha, K.-I. Ueda, H. Yagi, T. Yanagitani, and A. A. Kaminskii, "Yb3+:y2o3 ceramics - a novel solid-state laser material," *Japanese Journal of Applied Physics*, vol. 41, pp. L1373–L1375, December 2002.

[112] J. Kong, J. Lu, K. Takaichi, T. Uematsu, K. Ueda, D. Y. Tang, D. Y. Shen, H. Yagi, T. Yanagitani, and A. A. Kaminskii, "Diode-pumped yb:y[sub 2]o[sub 3] ceramic laser," *Applied Physics Letters*, vol. 82, no. 16, pp. 2556–2558, 2003.

[113] J. Kong, D. Y. Tang, J. Lu, and K. Ueda, "Spectral characteristics of a yb-doped y2o3 ceramic laser," *Applied Physics B*, vol. 79, pp. 449–455, 2004.

[114] N. Saito, S.-I. Matsuda, and T. Ikegami, "Fabrication of transparent yttria ceramics at low temperature using carbonate-derived powder," *Journal of the American Ceramic Society*, vol. 81, pp. 2023–2028, August 1998.

[115] J.-G. Li, T. Ikegami, and T. Mori, "Fabrication of transparent sc2o3 ceramics with powders thermally pyrolyzed from sulfate," *JOURNAL OF MATERIALS RESEARCH*, vol. 18, pp. 1816–1822, May 2003.

[116] J. G. Li, T. Ikegami, and T. Mori, "Solution-based processing of sc2o3 nanopowders yielding transparent ceramics," *JOURNAL OF MATERIALS RESEARCH*, vol. 19, pp. 733–736, March 2004.

[117] J. Lu, J. F. Bisson, K. Takaichi, T. Uematsu, A. Shirakawa, M. Musha, K. Ueda, H. Yagi, T. Yanagitani, and A. A. Kaminskii, "Yb[sup 3+]:sc[sub 2]o[sub 3] ceramic laser," *Applied Physics Letters*, vol. 83, no. 6, pp. 1101–1103, 2003.

[118] J. Lu, K. Takaichi, T. Uematsu, A. Shirakawa, M. Musha, K. Ueda, H. Yagi, T. Yanagitani, and A. A. Kaminskii, "Promising ceramic laser material: Highly transparent nd[sup 3+]:lu[sub 2]o[sub 3] ceramic," *Applied Physics Letters*, vol. 81, no. 23, pp. 4324–4326, 2002.

[119] A. A. Kaminskii, S. N. Bagayev, K. Ueda, K. Takaichi, A. Shirakawa, S. N. Ivanov, E. N. Khazanov, A. V. Taranov, H. Yagi, and T. Yanagitani, "New results on characterization of highly transparent nanocrystalline c-modification lu2o3 nanocrystalline ceramics: room-temperature tunable cw laser action of yb3+ ions under ld-pumping and the propagation kinetics of non-equilibrium acoustic phonons," *Laser Physics Letters*, vol. 3, no. 8, pp. 375–379, 2006.

[120] A. Gallian, V. V. Fedorov, S. B. Mirov, V. V. Badikov, S. N. Galkin, E. F. Voronkin, and A. Lalayants, "Hot-pressed ceramic cr2+:znse gain-switched laser," *Optics Express*, vol. 14, pp. 11694–11701, November 2006.

[121] D. Kracht, M. Frede, R. Wilhelm, and C. Fallnich, "Comparison of crystalline and ceramic composite nd:yag for high power diode end-pumping," *Optics Express*, vol. 13, pp. 6212–6216, August 2005.

[122] A. Strasser and M. Ostermeyer, "Improving the brightness of side pumped power amplifiers by using core doped ceramic rods," *Optics Express*, vol. 14, pp. 6687–6693, July 2006.

[123] J. Dong, A. Shirakawa, K. I. Ueda, H. Yagi, T. Yanagitani, and A. A. Kaminskii, "Ytterbium and chromium doped composite y[sub 3]al[sub 5]o[sub 12] ceramics self-q-switched laser," *Applied Physics Letters*, vol. 90, pp. 191106–191108, May 2007.

[124] J. Wisdom. PhD thesis, Stanford, 2007. Pending.

[125] C. Scott, M. Kaliszewski, C. Greskovich, and L. Levinson, "Conversion of polycrystalline al2o3 into single-crystal sapphire by abnormal grain growth," *Journal of the American Ceramic Society*, vol. 85, no. 5, pp. 1275–1280, 2002.

[126] W. D. Kingery and M. Berg, "Study of the initial stages of sintering solids by viscous flow, evaporation-condensation, and self-diffusion," *Journal of Applied Physics*, vol. 26, no. 10, pp. 1205–1212, 1955.

[127] G. N. Hassold, I.-W. Chen, and D. J. Srolovitz, "Computer simulation of final-stage sintering: I, model kinetics, and microstructure," *Journal of the American Ceramic Society*, vol. 73, no. 10, pp. 2857–2864, 1990.

[128] I.-W. Chen, G. N. Hassold, and D. J. Srolovitz, "Computer simulation of final-stage sintering: Ii, influence of initial pore size," *Journal of the American Ceramic Society*, vol. 73, no. 10, pp. 2865–2872, 1990.

[129] M. I. Peters and I. E. Reimanis, "Grain boundary grooving studies of yttrium aluminum garnet (yag) bicrystals," *Journal of the American Ceramic Society*, vol. 86, no. 5, pp. 870–872, 2003.

[130] I. Sakaguchi, H. Haneda, J. Tanaka, and T. Yanagitani, "Effect of composition on the oxygen tracer diffusion in transparent yttrium aluminium garnet (yag) ceramics," *Journal of the American Ceramic Society*, vol. 79, no. 6, pp. 1627–1632, 1996.

[131] D. J. Cherniak, "Rare earth element and gallium diffusion in yttrium aluminum garnet," *Physics and Chemistry of Minerals*, vol. 26, pp. 156–163, December 1998.

[132] T. A. Parthasarathy, T.-I. Mah, and K. Keller, "Creep mechanism of polycrystalline yttrium aluminum garnet," *Journal of the American Ceramic Society*, vol. 75, no. 7, pp. 1756–1759, 1992.

[133] M. Jimenez-Melendo, H. Haneda, and H. Nozawa, "Ytterbium cation diffusion in yttrium aluminum garnet (yag)-implications for creep mechanisms," *Journal of the American Ceramic Society*, vol. 84, no. 10, pp. 2356–2360, 2001.

[134] P. Shewmon, *Diffusion in Solids*, ch. 6, pp. 206–207. The Minerals, Metals and Materials Society, second ed., 1989.

[135] N. Matsushita, N. Tsuchiya, K. Nakatsuka, and T. Yanagitani, "Precipitation and calcination processes for yttrium aluminum garnet precursors synthesized by the urea method," *Journal of the American Ceramic Society*, vol. 82, no. 8, pp. 1977–1984, 1999.

[136] H. Yagi, J. F. Bisson, K. Ueda, and T. Yanagitani, "Y3al5o12 ceramic absorbers for the suppression of parasitic oscillation in high-power nd:yag lasers," *Journal of Luminescence*, vol. 121, pp. 88–94, November 2006.

[137] P. Shewmon, *Diffusion in Solids*. The Minerals, Metals & Materials society, second ed., 1989.